UNIVERSITÀ DEGLI STUDI
DI MODENA E REGGIO EMILIA

Dottorato di ricerca in Molecular and Regenerative Medicine
Ciclo XXXV

Development of combined cell and gene therapy for COL17A1-dependent Junctional Epidermolysis Bullosa

Relatore:
Prof. **Michele De Luca**

Correlatore:
Dott.ssa **Laura De Rosa**

Coordinatore del Corso di dottorato:
Prof. **Michele De Luca**

Candidata:
Ivanna Nesteruk

Anno Accademico 2021/2022

INDEX

ABSTRACT

Collagen 17 (COL17) is a transmembrane type II protein involved in genetic and autoimmune blistering skin diseases. Reduced levels or total absence of COL17 cause a subtype of Junctional Epidermolysis Bullosa (JEB), a group of rare genetic skin diseases characterized by insufficient anchoring of the epidermis to the dermis resulting in skin blistering, mucosal fragility, and increased risk of cutaneous carcinogenesis.

This project aimed at developing a combined cell and gene therapy for such a disease. To this end, we developed a self-inactivating γ retroviral vector (SIN-γRV) in which the *COL17A1* cDNA is under the control of the human elongation factor 1α short promoter (EF1α). A stable, GMP-compliant packaging cell line was established, and its performance in correcting JEB patients' cells was analyzed. At best, 76% of transduction efficiency was achieved. However, despite the VCN being 11, the expression of COL17 was low, not comparable to the healthy donors. Contemporary to the SIN-γRV, an γRV vector carrying *COL17A1* cDNA under the control of MLV long terminal repeat (LTR) promoter was studied, showing successful results in both the efficiency of transduction and the expression of COL17 in JEB keratinocytes with an average VCN of 3.

The SIN-γRV vector adopted in this project showed great results with other therapeutic genes, such as *COL7A1* causative of Dystrophic Epidermolysis Bullosa. This suggests intrinsic *COL17A1*-related expression issues in the SIN-γRV framework. A deep study of the SIN-γRV-transduced clones revealed that 20% of the integrated sequences consisted of rearranged forms of the therapeutic gene. Interestingly, rearrangements involved not only the *COL17A1* transgene but also the viral backbone. However, the presence of rearranged sequences only partially justifies the low expression of COL17 in transduced keratinocytes. A combination of events may explain this phenomenon. The analysis of splicing sites within the *COL17A1* ORF suggests the presence of strong splice donor/acceptor pairs that may be responsible for the low expression of the transgene. More data are necessary for a full understanding of the role of splicing in the SIN-γRV-*COL17A1* vector.

1 INTRODUCTION

The epidermis, the outermost layer of the skin, consists of a stratified squamous epithelium containing different cell types (keratinocytes, melanocytes, Langerhans' cells, and Merkel's cell) and serves as the body's initial barrier against pathogens and mechanical injuries [1]. Keratinocytes, the most prevalent cell type, are organized in distinct cellular layers [2]. The basal layer represents the epidermal proliferative compartment and contains stem cells and transient-amplifying (TA) progenitors [3-7]. Stable adhesion of basal epidermal keratinocytes to the basement membrane (BM) is vital to maintain skin integrity and relies on multiprotein complexes called **hemidesmosomes** [8, 9].

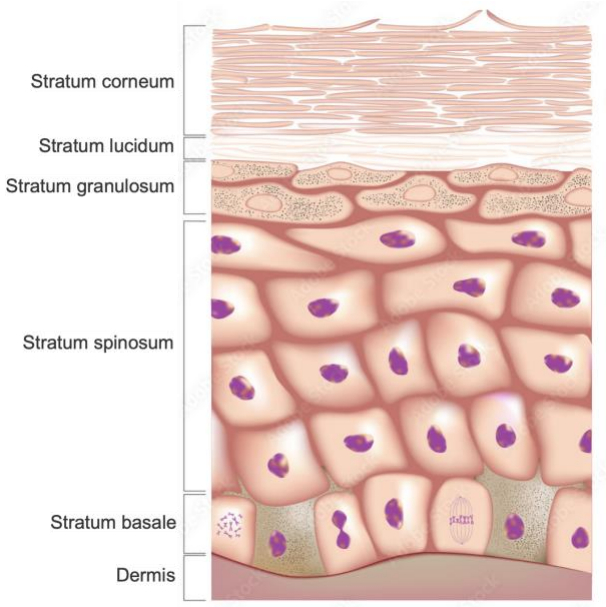

Figure 1. The basic structure of the human epidermis. Human epidermis consists of keratinocytes organized in different layers (indicated on the right) [1].

1.1 Structure of the hemidesmosomes

Hemidesmosomes (HDs) are highly specialized epithelial structures allowing basal keratinocytes to firmly adhere to the extracellular matrix. HDs sustain epidermal stability and mechanical strength by linking the keratin filament network to the basement membrane (BM), hence to the underlying dermis [9].

There are two types of hemidesmosomes that can be distinguished based on their protein components [10]. Type I HDs are found in stratified (and pseudostratified) epithelia, such as the epidermis, and consist of five major protein components: integrin α6β4, plectin isoform 1a (P1a), tetraspanin CD151, bullous pemphigoid antigen 1 isoform e (BPAG1e, also called BP230) and Collagen 17 (also called BP180 or BPAG2) (Fig.2) [11].

Type II HDs, found in simple epithelia such as that of the intestine, consist of integrin α6β4 and plectin and lack the two BP antigens [12, 13].

Ultrastructural examination of intact skin reveals HDs dispersed along the BM zone displaying a characteristic tripartite structure with inner and outer electron-dense plaques separated by a less dense zone [14-16]. Intermediate filaments (IFs) assembled by keratin 5 (K5) and keratin 14 (K14) associate with the inner plaque of HDs via binding to P1a and BPAG1e [17-19]. P1a and BPAG1e form critical links with transmembrane protein complexes that form the outer HD plaque and comprise integrin α6β4, Collagen 17, and CD151. Immediately beneath the basal keratinocyte plasma membrane lies the basal lamina, made of an electron-lucent zone, the *lamina lucida*, and an electron-dense layer comprising a closely packed fibrous network called the *lamina densa* (Fig. 2).

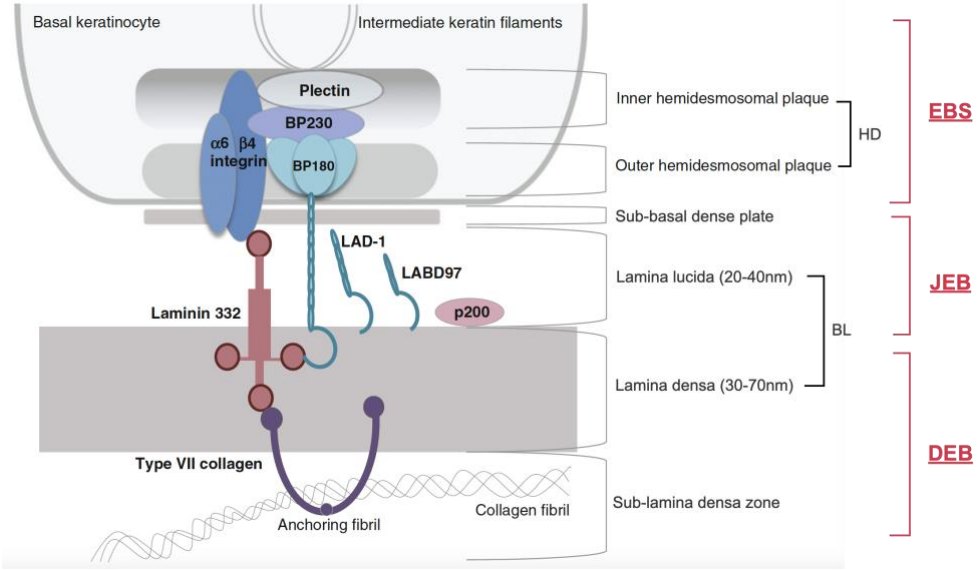

Figure 2. Schematic representation of a hemidesmosome. Outer brackets on the right indicate blister formation at different levels within the skin as is characteristic for the three major types of EB: EBS, within the epidermis; JEB, at the dermal-epidermal junction within the *lamina lucida*; DEB, in the upper layers of the dermis (adapted from Turcan et al., 2016).

1.2 Epidermolysis Bullosa

Inherited or acquired mutations in any of the HD components lead to a variety of rare genetic disorders collectively known as Epidermolysis Bullosa (EB) affecting approximately 30.000 individuals in Europe and 400-500.000 people worldwide. Functional impairment, reduction, or absence of HD proteins disrupt the epidermal-dermal junction. Indeed, hallmarks of EB are structural and mechanical fragility of the integuments that leads to unremitting skin blistering and erosions in response to minor trauma [20]. Massive chronic skin wounds greatly impair patients' quality of life, lead to recurrent infections and scars, and predispose patients to skin cancer [21-23]. Many EB subtypes can also have mucosal manifestations affecting other body sites (mouth, throat, esophagus, eyes) causing discomfort and difficulties in carrying out vital activities [24]. There is no cure for EB.

The genetic bases of EB have been deeply studied and a precise correlation between genetic defects and the different types of EB has been outlined [25, 26]. According to the mutated gene and the involved skin layer, EB can be classified into four basic subtypes (Tab.1):

- EB Simplex (EBS)
- Junctional EB (JEB)
- Dystrophic EB (DEB)
- Kindler EB (KEB)

All types and subtypes of EB are rare, with no racial or gender differences [27]. Transmission of EB is both autosomal dominant and autosomal recessive and may result in distinct clinical phenotypes.

Table 1. Classification of Epidermolysis Bullosa (EB) [26].

Level of skin cleavage	EB type	Inheritance	Mutated gene(s)
Intraepidermal	EB simplex	Autosomal dominant	*KRT5, KRT14* *PLEC* *KHLH24*
		Autosomal recessive	*KRT5, KRT14* *DST* *EXPH5 (syn. SLAC2B)* *PLEC*
Junctional	Junctional EB	Autosomal recessive	*LAMA3, LAMB3, LAMC2* *COL17A1* *ITGA6, ITGB4* *ITGA3*
Dermal	Dystrophic EB	Autosomal dominant	*COL7A1*
		Autosomal recessive	*COL7A1*
Mixed	Kindler EB	Autosomal recessive	*FERMT1 (syn. KIND1)*

1.3 Junctional Epidermolysis Bullosa

Junctional EB (JEB) is an ultra-rare disease, due to recessively inherited mutations in genes encoding for Laminin 332, Collagen 17, and Integrin α6, β4, and α3, marked by skin blistering occurring within the lamina lucida of the basement membrane (Tab.2). According to the USA register, JEB total incidence is just over two per million live births; the lower prevalence values reflect the short life expectancy of the severe form [20, 26].

The severity varies considerably across the two major subtypes, intermediate and severe, ranging from a normal life span with only minor skin affection, to death in the neonatal period, with severe skin and mucosal clinical manifestations [28]. While biallelic mutations in Laminin 332 give rise to either of these forms, biallelic mutations of the *COL17A1* and the α6β4 integrin genes result mostly in intermediate JEB phenotypes [29].

Table 2. Functional epidermolysis bullosa (JEB) clinical subtypes [26].

Most common JEB clinical subtypes	Targeted protein(s)
Severe	Laminin 332
Intermediate	Laminin 332
Intermediate	**Collagen 17**
Intermediate with pyloric atresia	Integrin α6β4
Localized	Laminin 332, **Collagen 17**, integrin α6β4, integrin α3 subunit
Inversa	Laminin 332
Late-onset	**Collagen 17**
LOC syndrome	Laminin α3A
With interstitial lung disease and nephrotic syndrome	Integrin α3 subunit

1.4 Collagen 17

Collagen 17 (COL17), also known as BP180/BPAG2, is a type-II-oriented transmembrane collagen composed of 3 identical 180-kDa α-chains [30].

COL17 is a central component of type I hemidesmosomes and plays a fundamental role in stabilizing the cell-stromal adhesion at the level of the basal lamina. Stabilization occurs by the projection of COL17 beneath hemidesmosomes mediating the linking of the keratin IFs to the anchoring filaments of the underlying dermis [31].

Each COL17 monomer consists of a globular cytosolic amino terminus of 466 amino acids (intracellular domain, ICD), a short membrane-spanning domain of 23 amino acids, and a large carboxy-terminal domain of 1008 amino acids (extracellular domain, ECD or ectodomain). ECD features 15 collagenous domains interspersed with non-collagenous (NC) ones [32]. The extracellular domain of COL17 can be physiologically cleaved from the cell surface by ADAM proteins in a process known as ectodomain shedding. COL17 shedding yields 120kDA and 97kDA soluble

peptides (also known as LAD-1 and LADB-97, respectively) that are incorporated into the extracellular matrix and are involved in the keratinocyte motility and basement membrane formation [33, 34]. In cultured keratinocytes, the soluble LAD-1 domain is detectable in the culture medium; mass spectrometry analyses have revealed that the cleavage occurs at different regions within the NC16A domain [33-37].

COL17A1-dependent Junctional Epidermolysis Bullosa

Nonsense, frameshift, or splicing mutations of *COL17A1* lead to the development of JEB, marked by the absence or reduction of COL17. Currently, more than 100 mutations have been reported, spanning the entire gene (Fig.3) [38]. Acquired JEB can be caused by autoantibodies to Collagen 17 [39, 40]. The disease is marked by painful blisters that develop either spontaneously or in response to minimal mechanical trauma and heal with atrophic hyperpigmented or hypopigmented scars. Mucosal involvement is variable but less severe than that in dystrophic EB. Additional extracutaneous complications include hair loss, nail loss or dystrophy, and enamel hypoplasia [41, 42]. Squamous cell carcinomas may develop in chronic wounds [22].

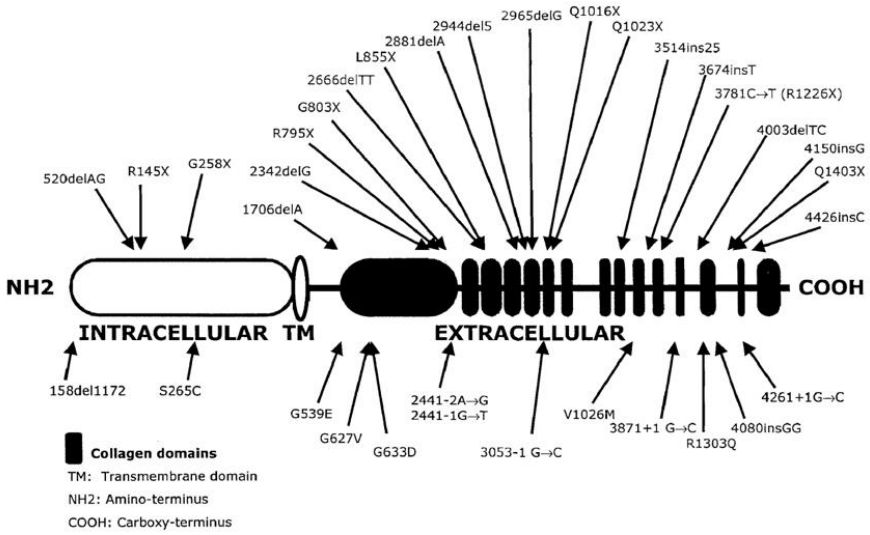

Figure 3. Overview of the mutations disclosed in the *COL17A1* gene. The arrows indicate the approximate position of mutations along the COL17 polypeptide chain. Mutations leading to stop codons are depicted above the polypeptide; all other mutations are shown below. The figure is not in scale [42, 43].

1.5 Therapeutic approaches

Currently, no curative therapy for EB is available; the treatment is palliative, consisting of symptom-relieving therapies based on wound management, painkillers, anti-inflammatory medications, and general supportive measures.

Considering the morbidity, the lethality of numerous subvariants as well as the current availability of only symptomatic treatment options, novel effective therapeutic approaches are urgently required.

Several strategies have been proposed to treat JEB:

- Aminoglycosides-mediated read-through approach
- Protein-based approach
- Cell and gene therapy approach

Aminoglycosides-mediated read-through approach

This approach consists of the repurposing of drugs belonging to the category of small molecules. In vitro experiments have shown that some of these drugs can induce premature termination codon (PTC) read-through in some RDEB and JEB-associated mutations, leading to the re-expression of a previously absent protein [44-48]. In particular, the antibiotic gentamicin has already been tested in a few patients with PTC mutations and seemed to improve the skin phenotype for a few months [49]. Clinical studies to test the effect of intravenous injections of gentamicin are currently conducted for RDEB (NCT03392909) and *LAMB3*-JEB (NCT03526159) [50]. Promising preclinical results were observed in *COL17A1*-JEB [47, 48].

Protein-based approach

The protein-based approach evolved from the awareness that COL17 can act as a cell-to-matrix sensor and dynamic modulator of keratinocyte motility and proliferation in cutaneous wound healing. In doing so, the extracellular domain of COL17 is of fundamental importance. Due to these properties, a therapy that envisages the delivery of the COL17 LAD-1 peptide has been proposed based on promising in vitro preliminary data collected from patients' skin equivalents [51].

Gene therapy approach

Aminoglycosides-mediated read-through approach and protein-based approach benefit from the ease of application, non-invasiveness, and relative cost-effectiveness; however, none of them can permanently restore the genetic defect of JEB patients, and no conclusive data on the clinical efficacy of these approaches are available.

Gene delivery mediated by retroviral vectors has the advantage of stable integration into the host cell genome allowing permanent reversion of the molecular defect underlying the disease.
This approach relies on the ex vivo transfer of a functional cDNA of the defective endogenous gene into target cells, which are then grafted back to the patient.

Gene therapy is an attractive concept, especially in disorders caused by mutations of single genes, and in that cases where target stem cells are accessible for in vitro manipulation and subsequent reinfusion/transplantation (Fig. 4).

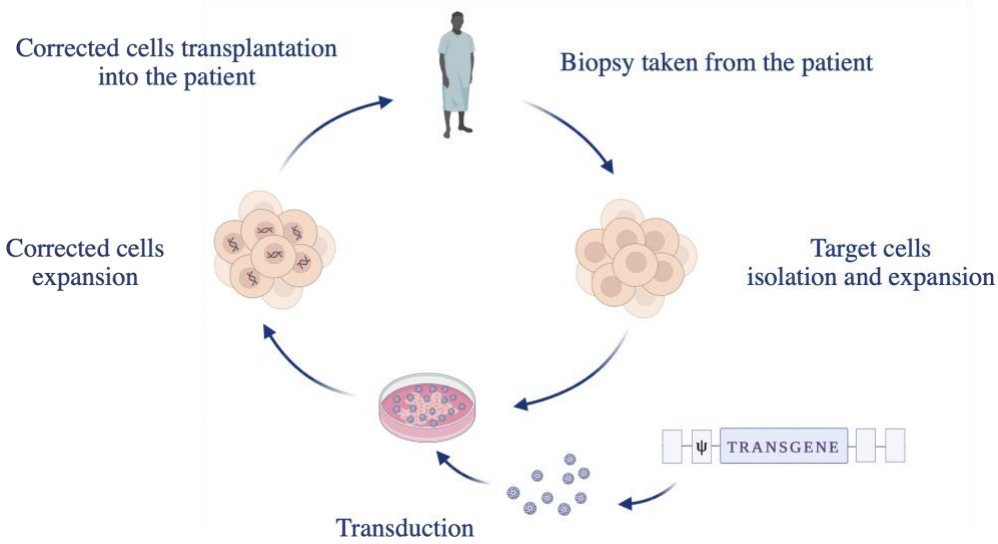

Figure 4. Schematic representation of a combined ex vivo cell and gene therapy.

Data generated from the clinical application of autologous cultures of epidermal cells provided conclusive evidence that cultivation and grafting procedures are safe and efficacious, and that permanent regeneration of both epidermal and corneal tissue can be achieved [52-56]. This paved the way for the development of combined cell and gene therapy for genetic skin diseases.

The first viral vector developed for gene therapy of different forms of EB was derived from the Moloney Leukemia Virus (MLV), a γ-retrovirus (γRV) that integrates into the host genome allowing permanent correction of the molecular defect underlying the disease [54, 57, 58].

Of note, the life of a 7-year-old boy suffering from a devastating form of *LAMB3*-dependent JEB was saved by combined cell and gene therapy strategy in which the patient's epidermal stem cells have been stably corrected with a MLV-derived γRV carrying the *LAMB3* cDNA [54].

A major concern about the employment of γRVs is the risk of insertional mutagenesis since they show a preferential integration pattern on actively transcribed genes, which can be potentially deregulated, as reported with hematopoietic stem cells [59-61]. Although γRV insertional mutagenesis events have never been reported in epidermal stem cells [54, 58, 62-65], the development of safer self-inactivating (SIN) γRV is anyway desirable.

SIN-γRVs are characterized by the lack of viral enhancers/promoters due to a deletion in the U3 region of the LTRs. Hence, in SIN-γRVs the expression of a target gene relies solely on an internal promoter. This confers a reduced risk for insertional mutagenesis and secondary cancer [61, 66]. SIN-γRVs have been shown to be as effective as the clinically used LTR-driven vectors [67, 68].

Moreover, the SIN design offers the possibility to choose the internal promoter according to specific requirements needed for a given application. Thus, the generation of SIN platforms creates a more efficient and possibly safer tool for gene therapy.

2 AIM OF THE PROJECT

The aim of this project was to develop a safe and efficacious SIN-γRV-*COL17A*1 able to tackle *COL17A1*-dependent JEB.

A similar vector was developed by our team for the treatment of Recessive Dystrophic Epidermolysis Bullosa (RDEB); this vector carries the *COL7A1* cDNA, driven by the human EF1α promoter. A stable viral packaging cell line, based on HEK293Vec® cells, was established in collaboration with BioNTech IMFS (Germany). Preclinical data assessing the performance of this viral vector showed successful correction of RDEB patient's cells (>90% of transduced cells), characterized by soaring expression of the therapeutic gene and physiological processing of COL17 (Fig.4). A clinical trial application is currently ongoing.

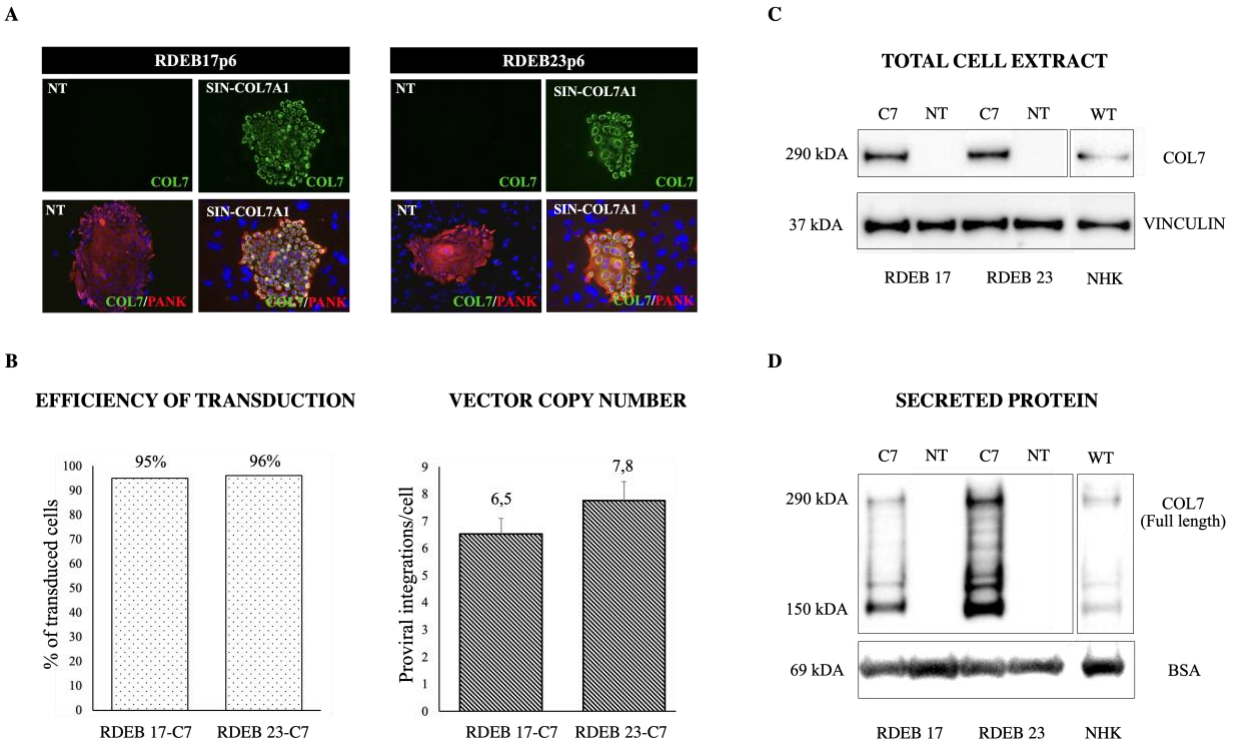

Figure 4. Preclinical data of combined cell and gene therapy for RDEB patients. A) Immunofluorescence performed on RDEB cells; B) Efficiency of transduction (left panel) and vector copy number (right panel) evaluation on corrected RDEB cells. C-D) Western blot analysis performed on C) cell lysates and D) on the conditioned media of RDEB samples. Of note, due to the low level of COL7 in wild-type (WT) samples, two different time exposures were used. Time exposure for RDEB lisates:11 seconds. Time exposure for wild-type lysates: 5 minutes. Vinculin exposure: 11 seconds for all samples. Time exposure for RDEB secreted protein:1 second. Time exposure wild-type secreted protein: 1 minute. BSA exposure: 1 second for all samples. Of note, SIN-COL7A1 stands for SIN-γRV-COL7A1.

3 RESULTS

3.1 Construction of self-inactivating retroviral vector

Human *COL17A1* cDNA (4494bp) was cloned into an exchange vector (pbib-ETAR-fcvi-ES-12-6(g)ps), under the control of the human Elongation Factor 1α short promoter (EF1α, 212bp). For an efficient regulation of *COL17A1* expression, its 5' UTR sequence has been cloned at the 5' of the transgene, while the woodchuck hepatitis virus post-transcriptional regulatory element (WPRE) was placed downstream.

The distinctive feature of this vector is the presence of Flippase and Cre recombinase-specific sequences that are necessary for its integration in the genome of the packaging cell line. The structure of the resulting construct, named pbib-*COL17A1*, is shown in Figure 5.

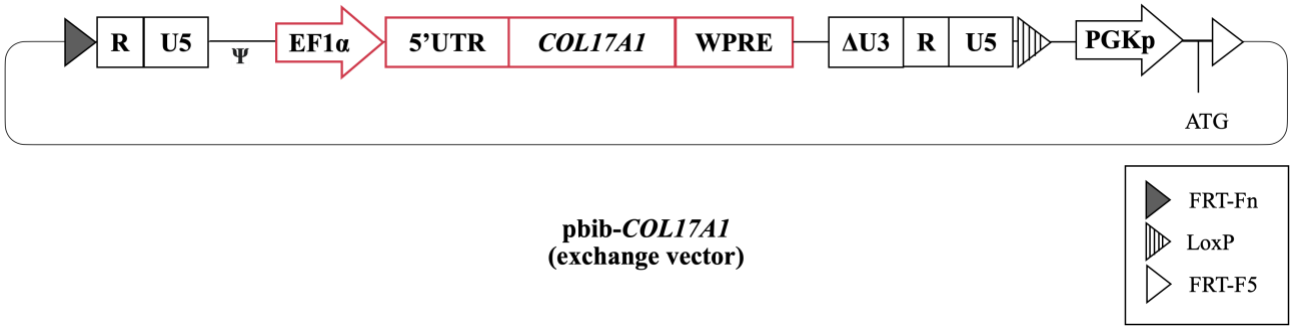

Figure 5. Pbib-*COL17A1* exchange vector design. Outline of the exchange vector bearing the *COL17A1* cDNA. The expression cassette is presented in red boxes. The picture is drawn not in scale.

3.2 Establishment of SIN-γRV-COL17A1 packaging cell clones

To produce clinical-grade MLV-based γRV, stable packaging cell lines are usually established relying on the mouse or human cell lines transduced with retroviral helper genes (gag, pol, and env) and the transfer vector (containing the therapeutic cDNA). These constructs integrate into the genome of the packaging cell and can be continuously expressed from the integrated provirus. The assembly of these components leads to the generation of γRV virions capable to infect target cells. These virions hold a linear RNA genome transcribed from the transfer vector, which is the only one bearing the encapsidation signal (Ψ), and hence, the only one being encapsidated.

Because of the deletion of the viral promoter in the U3 region, conventional generation of SIN-γRV packaging cells is no longer possible. A solution to this problem could be a site-directed integration of the vector encoding the therapeutic protein via recombinase-mediated cassette exchange (RMCE) into a predefined chromosomal locus of packaging cells. This method, based on Flippase (FLP) and

Cre-recombinase activity, would ensure a stable therapeutic vector production and well predictable viral titers [69].

We thus used this targeting system to generate a stable packaging cell line for both *COL7A1* and *COL17A1* (in collaboration with BioNTech IMSF, Germany).

293Vec-AMPHO® cells were used as starting material. These cells carry an amphotropic envelope protein, FLP and CRE-recombinase recognition sites, and a truncated neomycin resistance gene (promoter and start codon deleted) (Fig.6).

To generate the SIN-γRV producer clone for *COL17A1*, 293Vec-AMPHO® cells were co-transfected with the pbib-*COL17A1* exchange vector and FLP-recombinase mRNA. The presence of FLP inside the 293Vec-AMPHO® cells triggered the RMCE that induced the site-directed integration of the pbib-*COL17A1* exchange vector into the genome of the packaging cells (Fig.6), hence generating a stable packaging cell line that regularly releases into the culture medium viral particles pseudotyped with the amphotropic envelope.

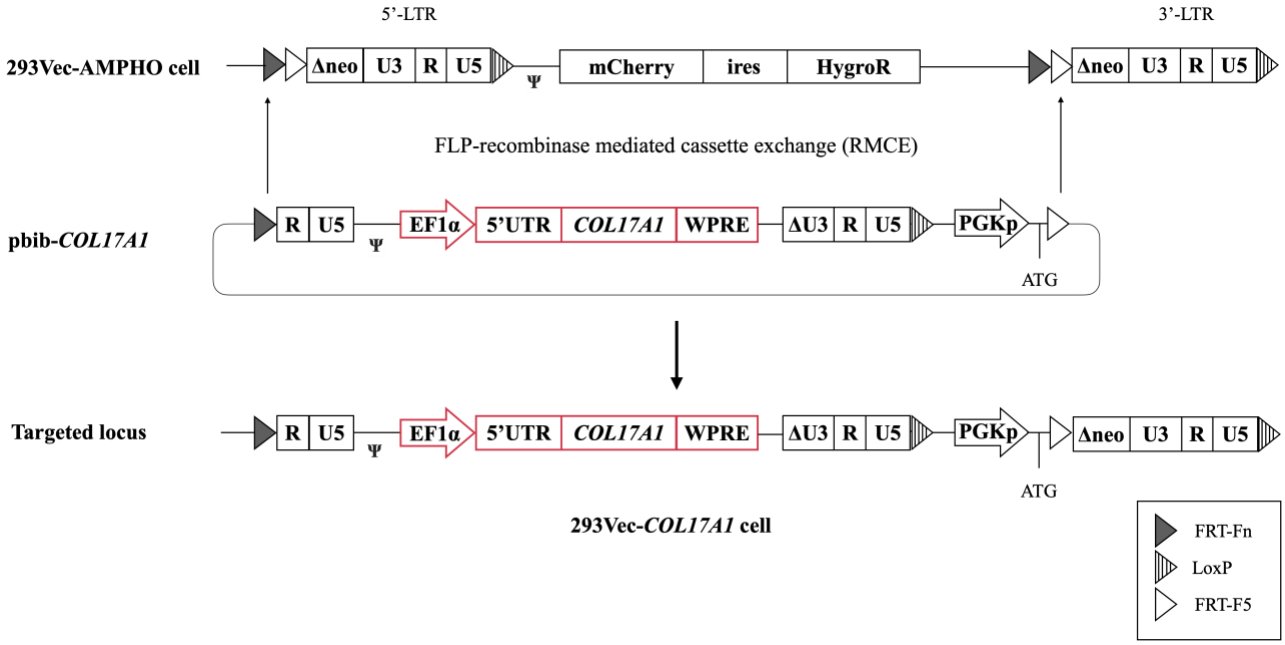

Figure 6. RMCE process inside the 293Vec-AMPHO® cells.

Upon the precise RMCE reaction, a loxP site, the constitutive PGK promoter, and a start codon are introduced in the packaging cell leading to the completion of the truncated neomycin resistance gene. Thus, only neomycin-resistant 293Vec-*COL17A1* cells can be selected.

Limiting dilution of the targeted mass culture was performed, and single clones were expanded and seeded for viral production. Titration of the harvested vector supernatants was performed on HeLa cells and three packaging cell clones (clone #1, #11, and #17), giving the highest viral titer, were selected for testing in primary keratinocytes (Fig. 7).

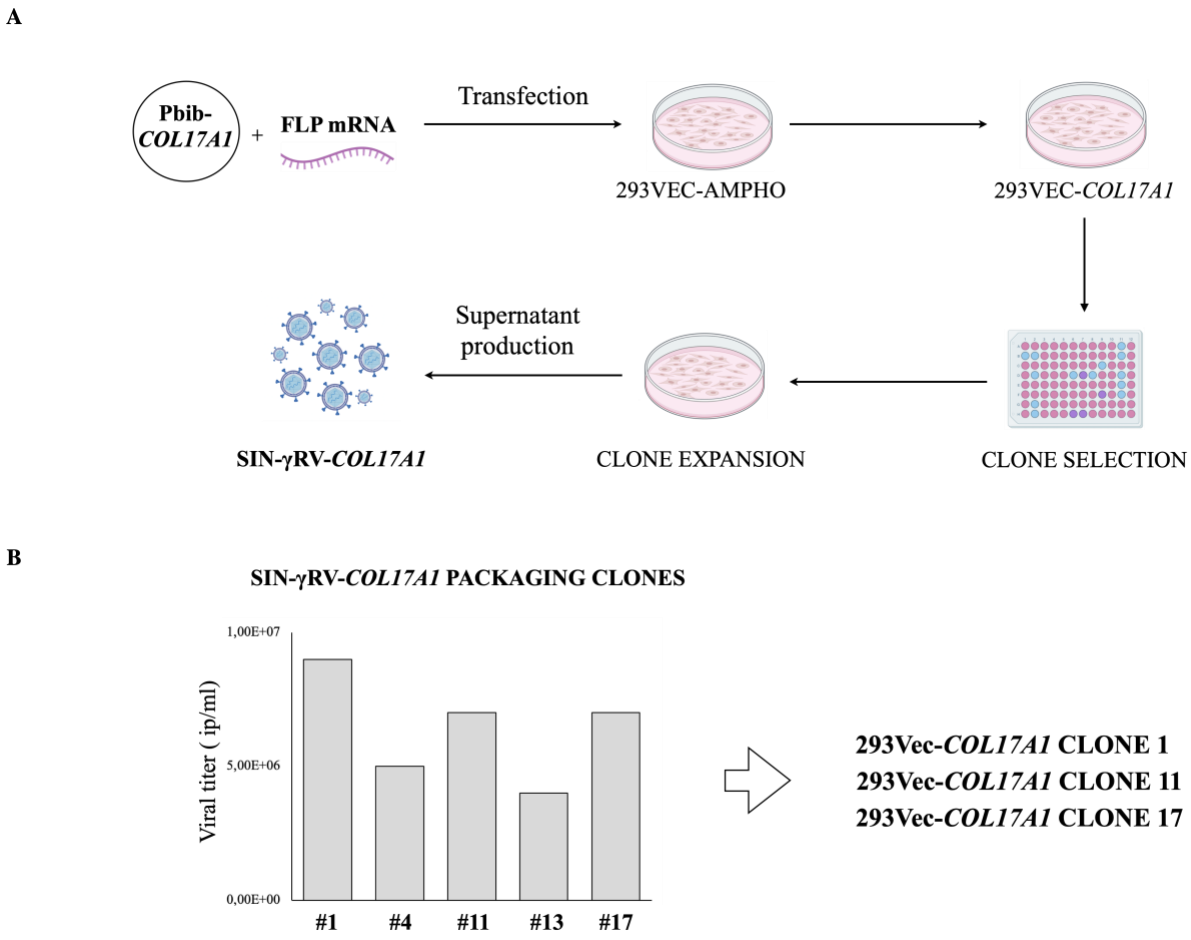

Figure 7. Establishment of 293Vec-*COL17A1* packaging clones. A) Workflow for the generation of the 293Vec-*COL17A1* packaging cell clones; B) Titration on HeLa cells of the viral supernatants derived from the packaging clones.

3.3 Study of vector supernatants performance in correcting COL17A1-JEB cells

To investigate the therapeutic potential of the selected packaging cell clones and their supernatants, *COL17A1*-JEB cells were transduced at a multiplicity of infection (MOI) 10.

Immunofluorescence performed on transduced keratinocytes revealed a variable transduction efficiency (51- 63%) for the three supernatants (Fig.8A).

The vector copy number (VCN), i.e., the average number of viral integrations per cell, was evaluated by real-time PCR using, as reference, a well-characterized clone carrying a single integrated proviral copy. VCN in transduced *COL17A1*-JEB keratinocytes was between 7,7 and 8,8 (Fig.8B). To preserve target cell genome integrity, the best clone would be the one with the highest transduction efficiency and the lowest VCN. Based on the results of these assays, **clone #1** was selected for further processing.

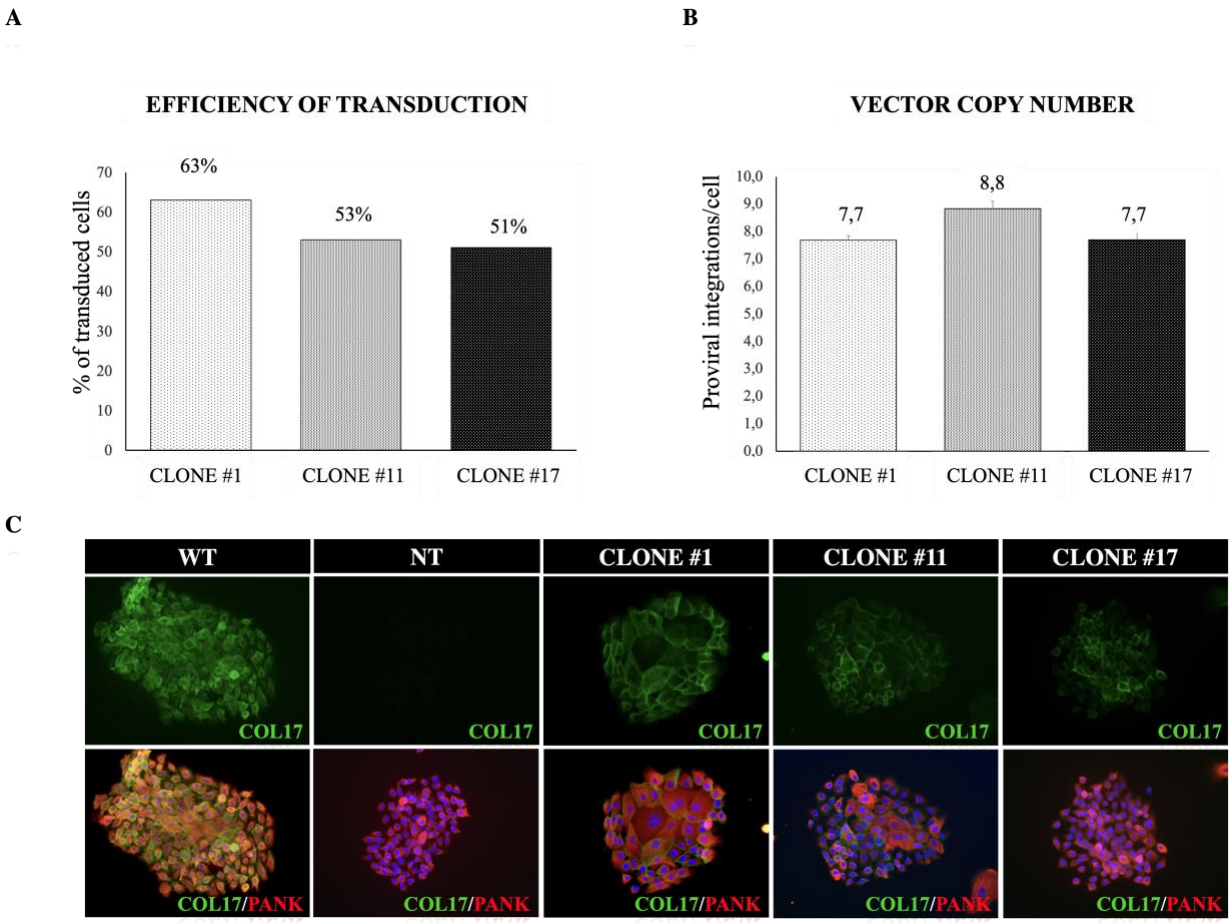

Figure 8. Study of vector supernatants performance in correcting *COL17A1*-JEB keratinocytes. A) Efficiency of transduction obtained with 293Vec-*COL17A1* clone #1, #11, and #17 supernatant. The percentage of transduced cells was manually counted by immunofluorescence on mass culture; B) VCN analysis was performed with real-time PCR on the genomic DNA of transduced bulk culture. Error bars represent standard deviation. C) Immunofluorescence analysis of COL17 expression (in green) JEB COL17-null keratinocyte transduced with 293Vec-*COL17A1* clone #1, #11, and #17 supernatant. Wild-type (WT) keratinocytes were used as a positive control. Pankeratin (PANK) was used to define keratinocyte colonies (in red).

3.4 Generation of the 293Vec-COL17A1 cleaned-up clone

While neomycin resistance allows an easy selection of the appropriate packaging cells, it cannot be used in transgenic keratinocytes destined for clinical application. Thus, a clean-up step aimed at removing the NeoR gene was introduced as a final step in the generation of the packaging clone. To this end, 293Vec-*COL17A1* Clone #1 cells were transfected with Cre-recombinase mRNA leading to the excision of NeoR sequences located between the two lox-P sites (Fig. 9).

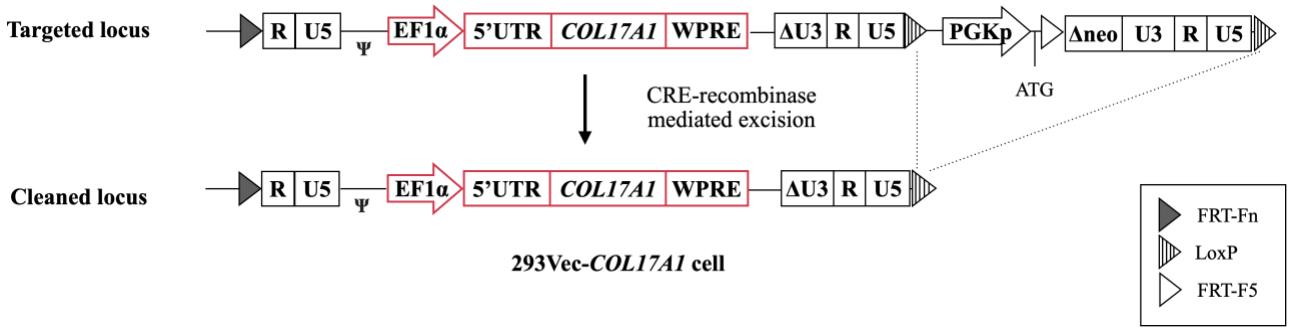

Figure 9. Graphic representation of the clean-up process inside the 293Vec-*COL17A1* Clone #1 cells.

The cleaned-up 293Vec-*COL17A1* Clone #1 cells were subcloned via limiting dilution, and a second clone selection was performed. Based on the highest titer, the supernatant of **clone #1.38** (Fig. 10) was chosen to transduce, at MOI 10, two *COL17A1*-JEB strains, JEB15 and JEB19, using RetroNectin as a transduction enhancer. In parallel, we transduced JEB15 and JEB19 cells with the same SIN-γRV carrying *COL7A1* cDNA (8.9 kb) at the same MOI. This control leverages the low level of endogenous COL7 protein in both wild-type and JEB samples allowing effortless detection of the *COL7A1* transgene expression.

A

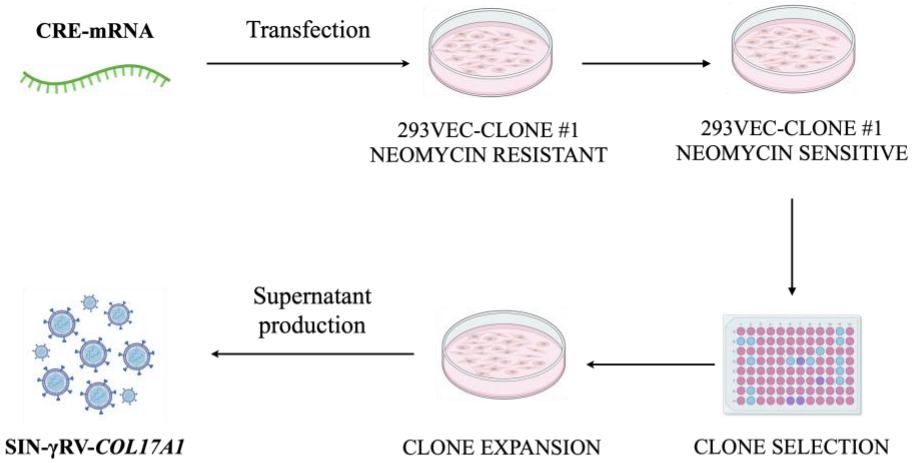

B

QC I: EVALUATION OF THE ABSENCE OF THE NEOMYCIN RESISTANCE GENE IN THE SELECTED CLONES

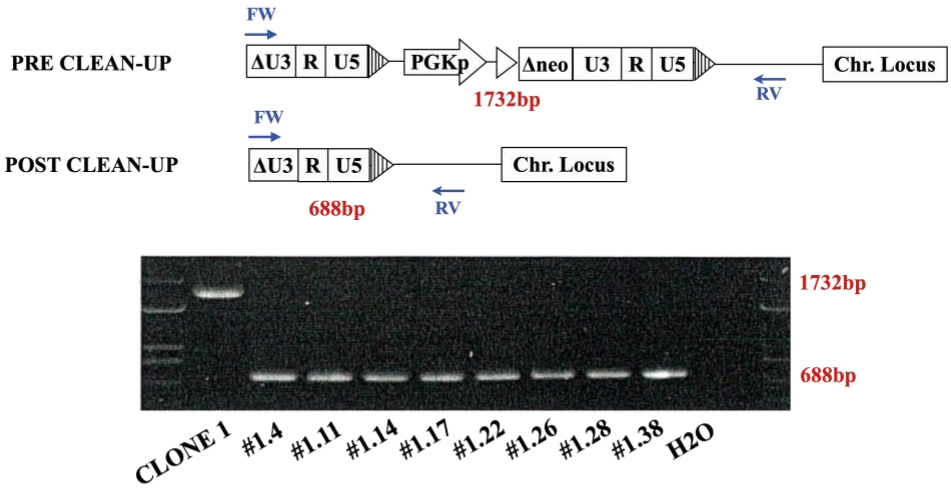

QC II: EVALUATION OF THE VIRAL TITER OF THE SUPERNATANTS OF THE SELECTED CLONES

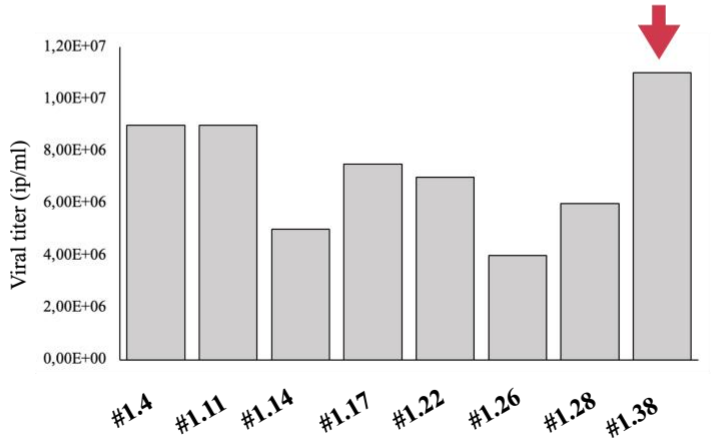

Figure 10. Selection of the final 293Vec-*COL17A1* packaging clone. A) The main points of the establishment of the final SIN-*COL17A1* packaging clone; B) Quality controls (QC) conducted during the selection of the final packaging clone. Upper panel: PCR amplification of the NeoR-containing fragment. Lower panel: titration on HeLa cells of the cleaned supernatants.

JEB15 and JEB19 strains showed 76% and 65% of SIN-γRV-*COL17A*-corrected cells, respectively (Fig. 11A). Transgenic keratinocytes showed a vector copy number of 11 (Fig. 11B). Nevertheless, we observed weak expression of COL17, highly heterogeneous among the different colonies, and rarely comparable to the expression of COL17 in wild-type keratinocytes (WT) (Fig. 11C). In contrast, even though *COL7A1* cDNA is twice as big as *COL17A1*, the SIN-γRV-*COL7A*1 was more successful in transducing target cells. About 90% of transduction efficiency was achieved in JEB15 and JEB19 cells, with an average of 5 integrated proviral copies/cell (Fig.11). Bright and homogeneous COL7 staining was observed in the mass culture by immunofluorescence (Fig.11), and the high COL7 expression was confirmed by western blot analysis (Fig. 12).

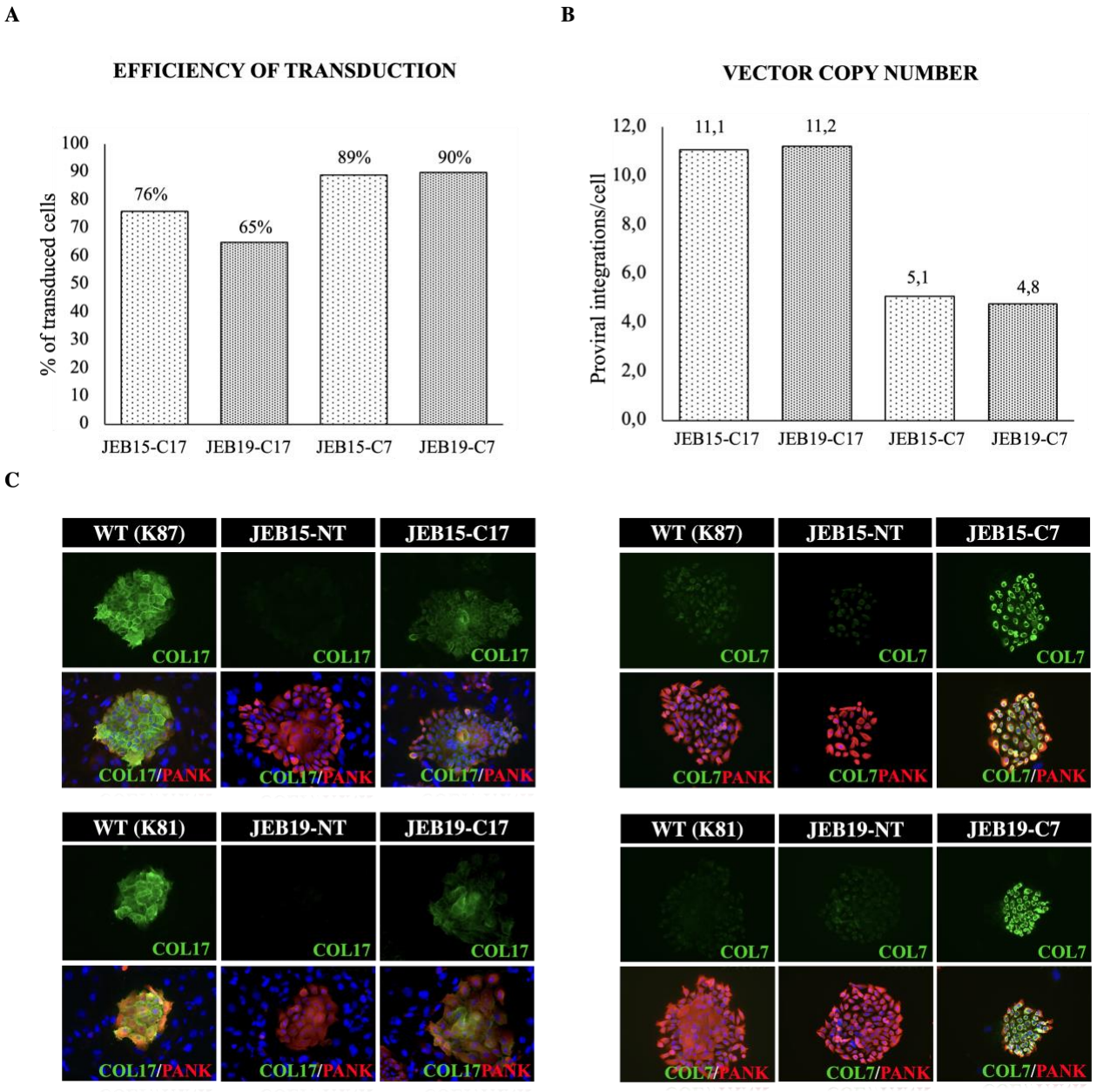

Figure 11. Evaluation of genetic correction of primary *COL17A1*-JEB keratinocytes. A) Efficiency of transduction of patients' keratinocytes one passage after transduction (passage 6). The percentage of transduced cells was manually

counted by immunofluorescence on mass culture; B) VCN analysis was performed via real-time PCR on the genomic DNA of the transduced mass cultures. Error bars represent standard deviation. C) Immunofluorescence analysis of the COL17 and COL7 expression in transduced cells. Wild-type (WT) cells were used as a positive control. Pankeratin (PANK) was used to define keratinocyte colonies (in red).

In contrast, Western blot analysis performed using cell lysates prepared from JEB15 and JEB19 transgenic cells revealed very low expression of COL17, confirming the immunofluorescence data. Both WT and transduced samples generated two principal bands corresponding to full-length collagen 17 (180kDa) and the cleaved extracellular peptide (120kDa), but these bands were more expressed in WT keratinocytes than in transgenic JEB 15 and JEB 19 cells. A 150kDa band was also detected, indicating presumably the pro-collagenous immature form of COL17. Strikingly, the same cells transduced with the same SIN-γRV carrying the cDNA of a different gene, *COL7A1*, showed a higher expression of COL7, as compared to the healthy donor. The collected data suggest that the SIN-γRV-*COL17A*1 is in fact unsuitable for a gene therapy approach.

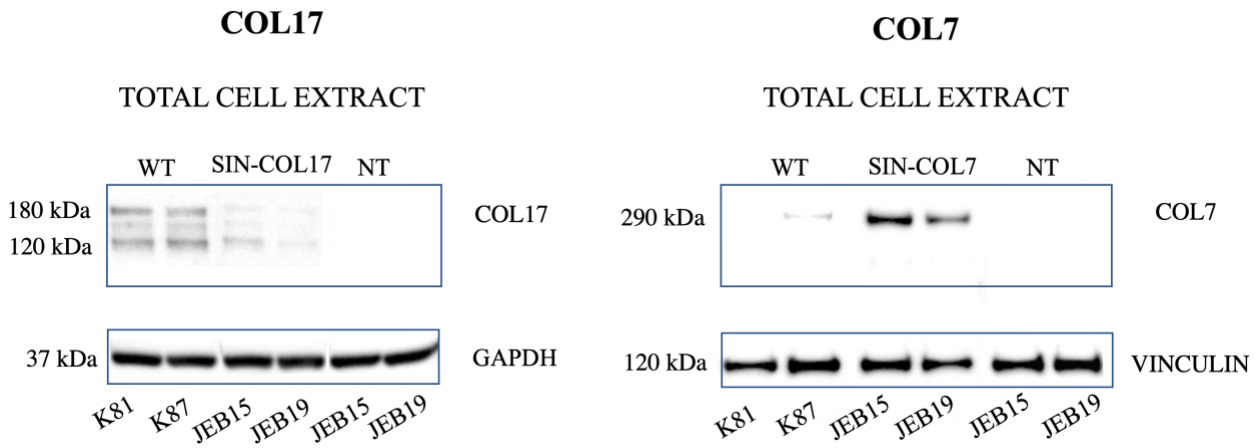

Figure 12. Western blot analysis. Wild-type keratinocytes, non-treated *COL17A1*-JEB cells (NT), and transduced *COL17A1*-JEB cells were investigated to produce type 17 and type 7 collagen. N.B. The low expression of COL7 in primary keratinocytes makes quite difficult the detection of endogenous protein by western blot. Of note, SIN-COL17A1 and SIN-COL7A1 stand for SIN-γRV-COL17A1 and SIN-γRV-COL7A1, respectively.

3.5 γRV-COL17A1 performance evaluation

We thus transduced JEB15 and JEB19 cells with an γRV in which *COL17A1* expression is driven by the LTR of the viral vector (γRV-*COL17A1*). The transduction was performed by the co-culture method relying on a stable AM12-*COL17A1* packaging cell line (see Materials and Methods, par. 5.2). Globally, the γRV-*COL17A1* vector showed higher transduction efficacy as compared to the SIN-γRV counterpart: 92% and 79% of correction were achieved in JEB15 and JEB19, respectively. γRV-transduced keratinocytes had an average of 3,3 integrated provirus copies per cell and bright and homogeneous immunofluorescence staining of COL17, virtually indistinguishable from the positive control, was observed (Fig. 13). Western analysis of cell lysates revealed that, despite the

restrained VCN, γRV-transduced cells express a considerably higher amount of COL17 as compared to the wild-type samples or SIN-γRV-transduced keratinocytes. This is likely due to the strong promoter activity of the γRV-LTR. Conditioned media analysis revealed two bands in both wild-type and transduced samples, at 120kDa and 97kDa: these bands represent the LAD-1 and LADB-97 cleaved forms of COL17, constantly and physiologically released by basal keratinocytes and are associated with correct basement membrane formation in the skin. Western blot signal intensity was quantified using ImageJ (Fig.13E). As shown in Figure 13E, the expression of the transgene in SIN-γRV-*COL17A1* transduced cells was three to nine-fold lower than that of wild-type sample and 15 to 37-fold lower than that of compared to the γRV-*COL17A1* transduced cells. Taken together, these data indicate that γRV-*COL17A1*, but not SIN-γRV-*COL17A1*, is suitable for its translation into clinics.

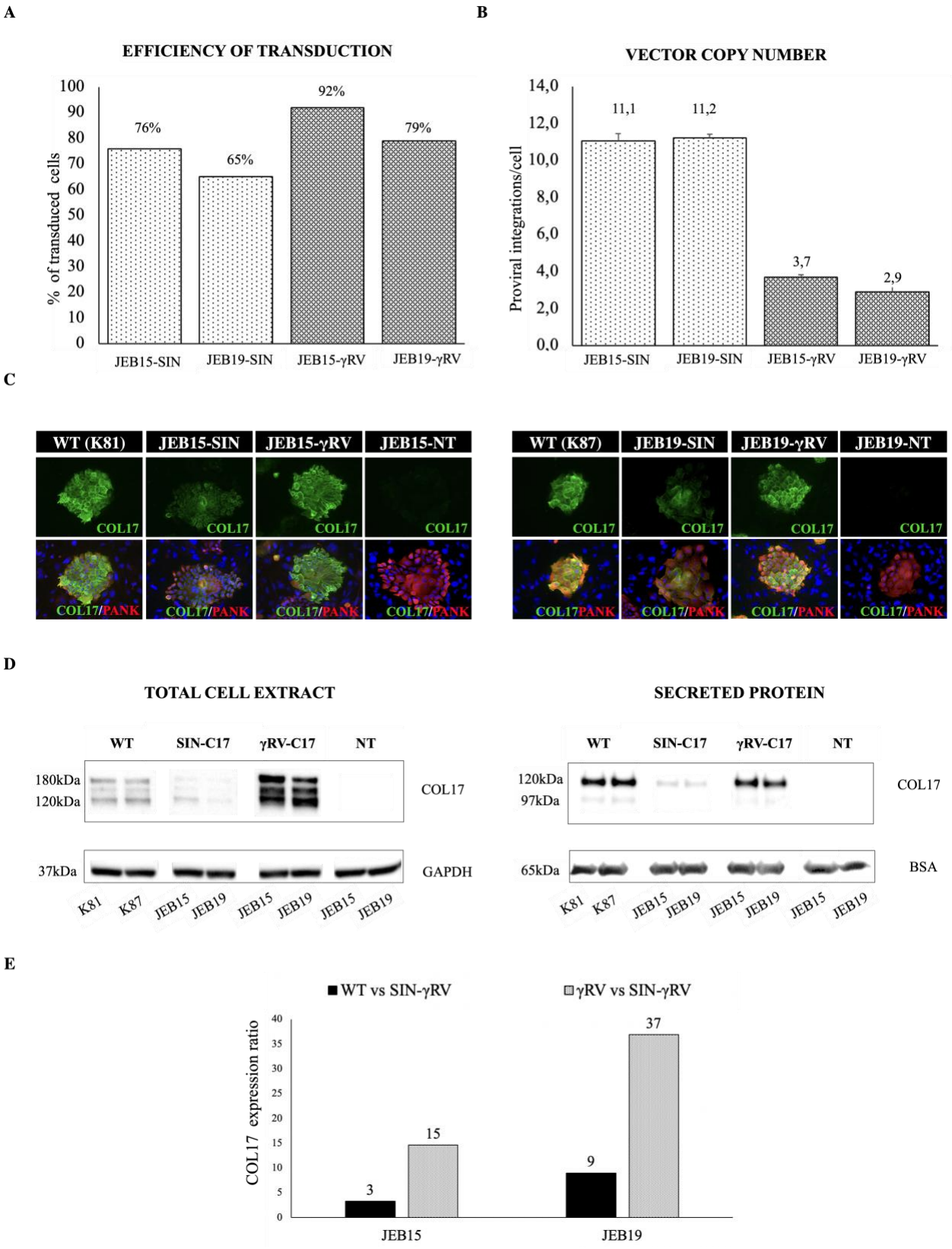

Figure 13. Comparison of γRV-*COL17A1* and SIN- γRV-*COL17A1* vector performance in primary *COL17A1*-JEB keratinocytes. A) Efficiency of transduction of target cells one passage after transduction (passage 6). The percentage of transduced cells was manually counted by immunofluorescence on mass culture. B) VCN analysis was performed via real-time PCR on the genomic DNA of the transduced bulk cultures. Error bars represent standard deviation. C) Immunofluorescence assessing the expression of COL17 in transduced cells. D) Western blot analysis on the cell extracts and the exhausted media of healthy, wild-type keratinocytes (WT) and *COL17A1*-JEB cells; E) COL17 expression ratio calculated by ImageJ. COL17 band intensity given by the lysates of WT samples and γRV-transduced samples was compared to the COL17 band intensity given by the lysates of SIN-transduced samples.

3.6 Analysis of the expression cassette integrity

Our findings indicate that a high number of SIN-γRV-*COL17A1* integrate into the genome of the target keratinocytes, but they are not able to properly express COL17. To investigate the presence of transgene rearrangements, a clonal analysis was carried out. Limiting dilution of the SIN-γRV-*COL17A1* transduced JEB15p6 bulk culture was performed, and single colonies were analyzed for the integrated sequence of the gene of interest (Fig.14). A total of 120 clones were examined: genomic DNA was used as the template for the PCR amplification of the expression cassette and the size of the resulting band was compared to the size of the pbib-*COL17A1* plasmid.

Interestingly, the efficiency of transduction evaluated by PCR was 94%, instead of the 76% measured through immunofluorescence analysis. Among the transduced clones, 20% showed *COL17A1* sequence rearrangements (smaller *COL17A1* bands). Sanger sequencing done on rearranged clones revealed that the rearrangement events mainly occur in the extracellular domain of *COL17A1* and involve large portions of the transgene (up to 1000bp). In addition, 9% of the rearrangements involved the viral backbone beyond the expression cassette.

An analogous experiment was performed on MLV-corrected cells; the rearrangement rate was about 10%, indicating that, at least in part, these events are likely to occur in *COL17A1* cDNA sequence.

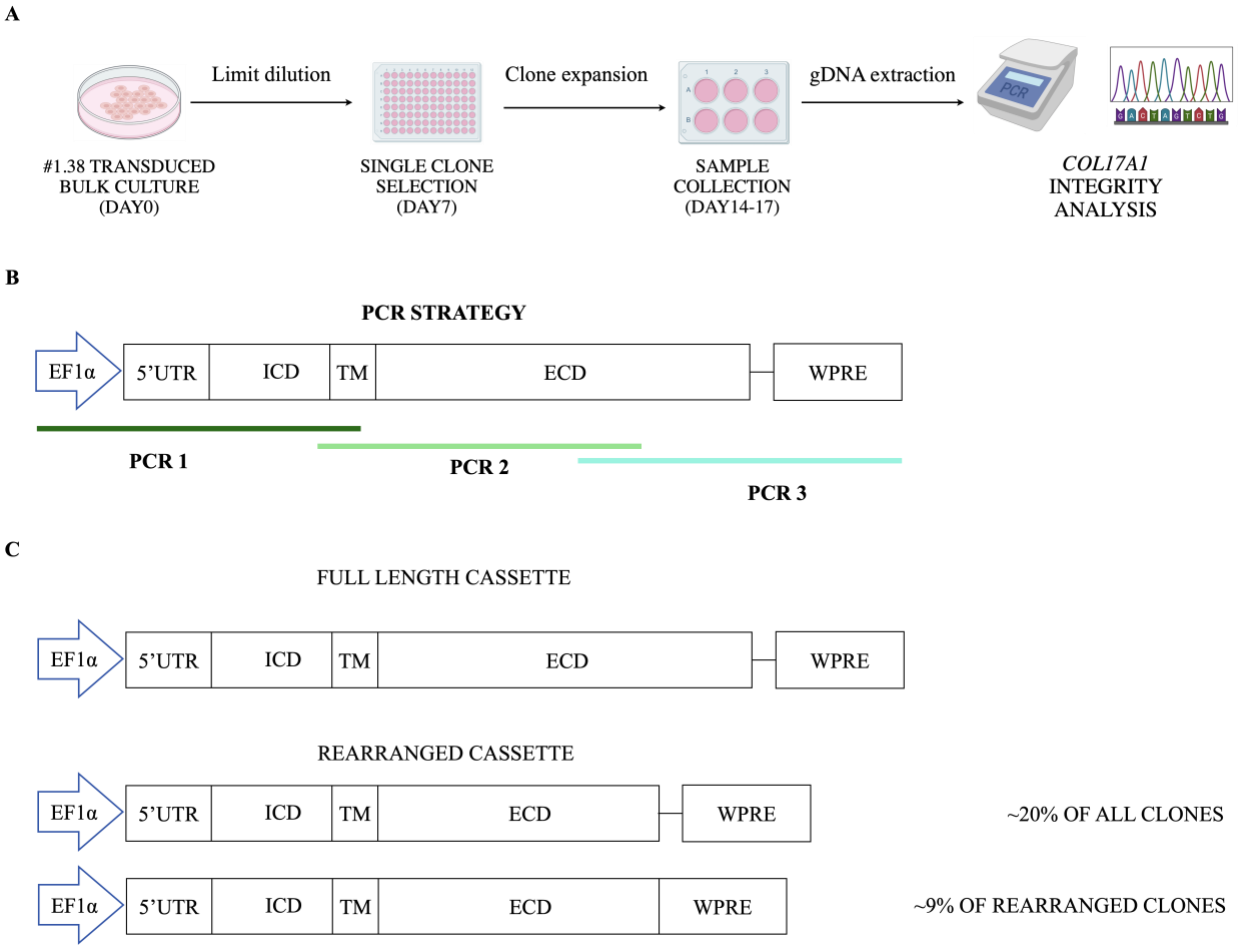

Figure 14. Determination of integrated sequence rearrangements in transduced clones. A) Design of the experiment; B) Representation of the PCR strategy adopted for the analysis of the expression cassette integrity. Due to the extension of the expression cassette (approximately 5.3 kb), three primer pairs were used; C) Schematic representation of the PCR and sequencing results of the *COL17A1* expression cassette in transduced clones. The picture is drawn not in scale.

3.7 Unraveling SIN-γRV-COL17A1 expression hurdles

To address the *COL17A1* expression issues, we adopted a two-fold approach: a promoter-based approach and a transcripts-based approach.

Promoter-based approach

In the promoter-based approach, the EF1α promoter was replaced by the human promoter of Keratin 14, a strong tissue-specific promoter. Keratin 14 (K14) is one of the major proteins expressed by the basal cells of the epidermis and is abundantly transcribed in cultured human keratinocytes. For these reasons, the K14 promoter is an attractive candidate for use in keratinocyte-mediated gene therapy. In the present study, we explored the potential of using the human K14 promoter to drive *COL17A1* expression. To this end, the K14 full promoter was cloned upstream the *COL17A1* ORF into the pSRS

vector, an MLV-based SIN-γRV suitable for transient virus production. As a control, the EF1α-*COL17A1* construct was cloned in the same vector.

Transcripts-based approach

In the transcripts-based approach, the possibility of aberrant splicing was investigated by PCR, using two specific primers that bind the 5'UTR (forward primer) and the TGA (primer reverse) to detect either the vector-derived transcript or the endogenous transcript (Fig.15). The SIN-γRV-transduced samples presented multiple *COL17A1* transcripts, while γRV-transduced samples and the wild-type samples were characterized by fewer (or no) alternative transcripts. Of, note alternative transcripts are also detected in the non-transduced JEB15 cells, likely due to its *COL17A1* mutation. But even so, endogenous *COL17A1* transcripts represent a common background for both SIN- γRV- and γRV-transduced samples.

The viral constructs (SIN-γRV-*COL17A1* and γRV-*COL17A1*) are identical except for the nature of their promoters (EF1α and LTR, respectively), which seem to be the key element that determines the differences in the expression of COL17 and the processing of the mRNA.

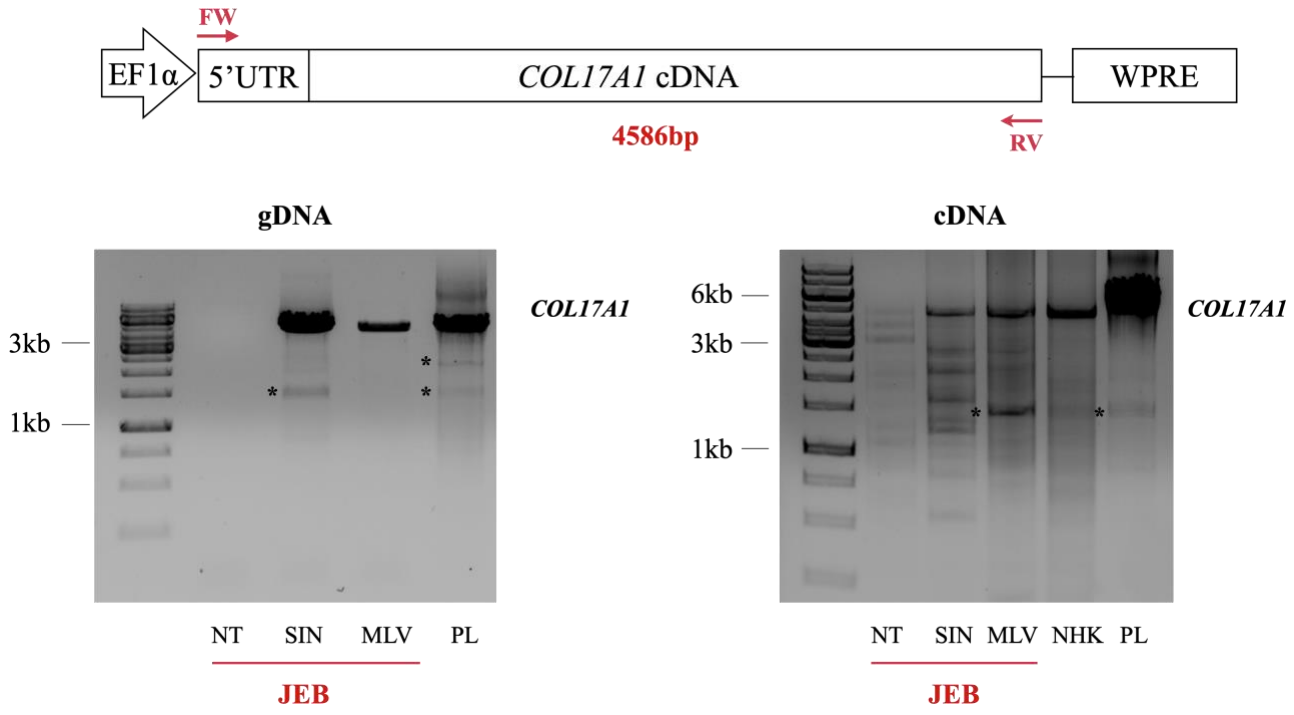

Figure 15. Study of the *COL17A1* transcripts. Amplification of the *COL17A1* cDNA from the genomic DNA (gDNA) and the cDNA of transduced JEB15p6 cells. Pbib-*COL17A1* plasmid (PL) was used as a reference for the size of the bands. Asterisks mark nonspecific PCR bands.

To confirm the propensity of *COL17A1* splicing, particularly in SIN-γRV-transduced cells, a bioinformatic prediction of the splicing process was performed using four different tools (Alternative

Splice Site Predictor, NetGene2, Berkeley Drosophila Genome Project, and Spliceator). The prediction outputs confirmed the presence of strong splice donor-acceptor pairs within the *COL17A1* ORF that may be responsible for non-functional viral particles and the large number of putative transcripts observed in Fig. 15 (Fig. 16A, B). A site-directed mutagenesis strategy was designed to eliminate the splice donor site SD2223, which was identified in all bioinformatic predictions as one of the strongest splice sites. The mutagenesis was performed without alteration of the amino acid sequence (Fig.16 C). The mutagenized *COL17A1* sequence (*COL17A1* SD2223*) was cloned into the pSRS SIN-γRV.

A

Donor Site Predictions

Start	END	Sequence	Score
84	98	ggctatggtatggat	0,43
1559	1573	ggaggaggtgaggaa	0,76
1803	1817	cctaaaggtgacatg	0,59
1857	1871	actccaggtatccct	0,79
1983	1997	cctcgtggtgaggca	0,86
2214	2228	cccaaaggtgaccag	0,77
2223	2237	gaccagggtgagaaa	0,97
2286	2300	gctgttggtgagccc	0,64
2349	2363	ccaagaggtgaacaa	0,66
2457	2471	cttcccggtaccct	0,57
2484	2498	ataaaaggtgaacca	0,53
2592	2606	cctccaggtgcccca	0,42
2973	2987	ccaaaaggtgacaaa	0,79
2982	2996	gacaaaggtgatccg	0,49
3052	3066	gtaccatgtacgtgt	0,88
3301	3315	cttcggggtacggtg	0,83
4443	4457	cccaaaggtgacagg	0,72
4470	4484	ccaccaggtcatcct	0,43
4524	4538	gacaaaggtgaccaa	0,52

Acceptor Site Predictions

Start	END	Sequence	Score
314	354	tgcctccacctctagttacaggagggctcactcacctgcct	0,72
355	395	ccactctgcccaactccccaggctcaaccttgaaaggaaa	0,65
1225	1265	ctgggcccttgggccacccaggtccacaaggaccaaagggt	0,91
1870	1910	ctgggcccttgggccacccaggtccacaaggaccaaagggt	0,81
2056	2096	atggcccacctggtgtcccaggttctgtgggtcccaaaggt	0,62
2100	2140	agcggctctcctggcccacagggccctccaggtcctgtagg	0,65
2119	2159	agggccctccaggtcctgtaggtctccaagggctccgaggt	0,58
2533	2573	catcgatgctcactgtcccaggcccccccaggacctcctgga	0,65
2692	2732	caccagggccttccattccaggcccaccaggaccccgaggc	0,89
2797	2837	ccttcctctccggccccccaggcccacctggcccccaggt	0,94
2815	2855	caggcccacctggcccccccaggtcccaagggagaccaaggt	0,89
2922	2962	tctttcggactcaaccttcagggaccaccaggcccacctgg	0,42
3328	3368	cgtcctccatctcttctgaagacatcctggctgtgctgcag	0,76
3715	3755	ccggcttgtcattcatcccaggccctccaggacctcctggt	0,96
3742	3782	caggacctcctggtccccaggcctcgagggcccccgggt	0,91
3874	3914	gcttcattgttggcccccccaggccctcctgggccgcaggga	0,91
3891	3931	ccaggccctcctgggccgcagggaccccctggggacagccg	0,83
3965	4005	tagcagctcctcctcacacagctcatctgtcaggcggggca	0,75
4331	4371	caaggtcttctctgcctacagcaacgtgactgcggacctca	0,91

B

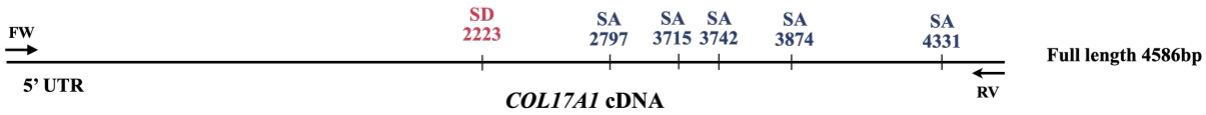

SPLICE VARIANTS THAT MAY EXIST (only scores >0,9 considered)

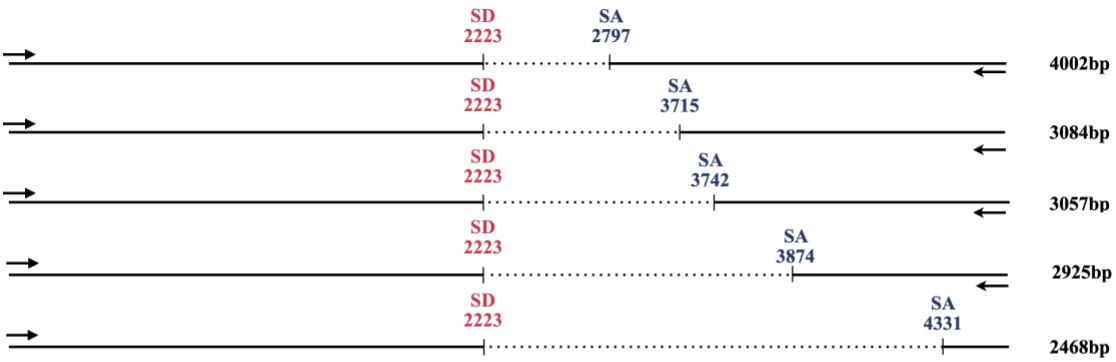

C

SD 2223 MUTAGENESIS

SD2223 **5' AAAGGTGACCAGGGAGAGAAAGGAC 3'** ***COL17A1-cDNA WT***

SD2223 **5' AAAGGTGACCAGGGTGAGAAAGGAC 3'** ***COL17A1-cDNA SD2223****

Figure 16. Bioinformatic prediction of *COL17A1* splice sites. A) Splice site prediction outcomes from the Berkley Drosophila Genome Project (BDGP); B) Schematic representation of splice variants that may exist upon the usage of

SD2223 site (red) and strong SA sites (blue); C) SD2223 mutagenesis strategy. Of note, the splice sites were named after the start nucleotide identified by the prediction algorithm.

3.8 Evaluation of pSRS-COL17A1 constructs in GABEB cells

The pSRS-*COL17A1* vector carrying the promoter change and the SD2223 mutation was used for transient viral vector production in 293 PHOENIX-AMPHO cells. As a control, the γRV-*COL17A1* supernatant from AM12-*COL17A1* cells was collected, concentrated, and used according to the protocol used for pSRS-*COL17A1* vectors.

Supernatants containing SIN-γRV produced by transient transfection were characterized by low viral titers (~10^5 ip/ml) which represents an important limit for the transduction of primary keratinocytes since the MOI must be calculated considering both keratinocytes and feeder layer 3T3-J2 cells. To overcome this hurdle, we adopted GABEB cells, immortalized COL17-null keratinocytes that do not necessitate feeder layer cells to grow.

GABEB cells were infected at MOI 3 with the supernatants carrying the different configurations of the *COL17A1* expression cassettes. RetroNectin® was used as a transduction enhancer. Transduction efficiency resulted to be quite comparable among all samples, thus absolute levels of Collagen 17 were compared by western blot assay.

Consistent with our previous findings on primary keratinocytes, the MLV-derived vector confirmed the high and successful COL17 expression with the lowest VCN value (VCN=1,4).

The K14 full promoter did not show any improvement in COL17 expression which was even lower as compared to the EF1α promoter. Conversely, the SD2223 mutation caused a slight increase in COL17 expression that could be attributed to the higher efficiency of transduction (47%).

More data are necessary for a full understanding of the role of splicing in the SIN- γRV-*COL17A1* and to perform a codon optimization to avoid any cryptic splicing sites.

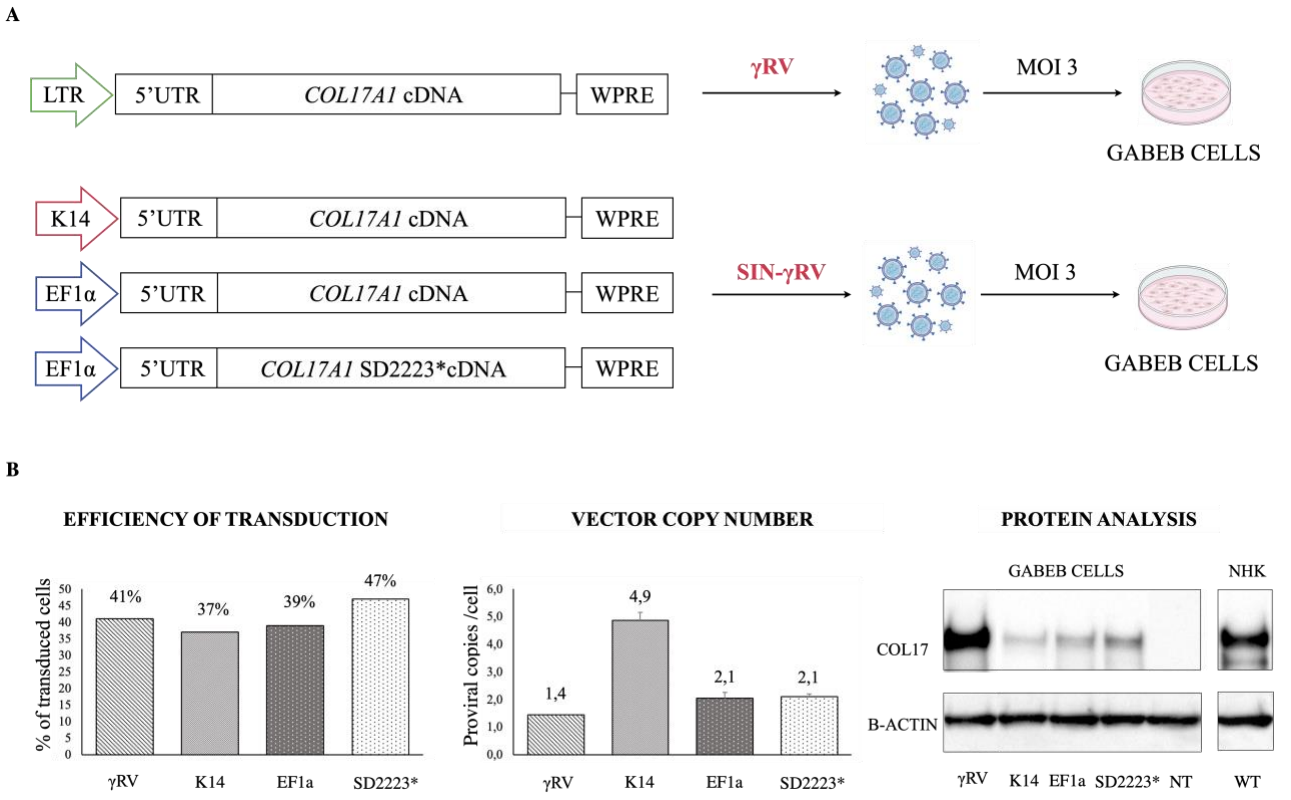

Figure 17. Self-inactivating retroviral vectors. A) Schematic representation of the developed pSRS-*COL17A1* SIN-γRVs carrying the modifications of the *COL17A1* expression cassette; B) Experimental outcomes obtained in GABEB cells, transduced at MOI 3. Left panel: percentage of transduced cells manually counted by immunofluorescence on mass culture. Middle panel: VCN analysis performed with real-time PCR on the genomic DNA of transduced bulk culture. Error bars represent standard deviation. Right panel: western blot analysis of COL17 expression in GABEB cells. Wild-type keratinocytes (WT) cells were used as a positive control.

4 DISCUSSION

In this work, we aimed at developing a combined cell and gene therapy for *COL17A1*-dependent JEB. Two different viral vectors were developed: a SIN-γRV-*COL17A1* and an γRV-*COL17A1* vector. Limited transduction efficacy was observed with the SIN-γRV-*COL17A1* vector; in the best case, only 76% of the *COL17A1*-JEB keratinocytes resulted to be corrected upon transduction, not sufficient to establish a gene therapy approach. In fact, in a gene therapy medicinal product, the percentage of the corrected cells must be >90% to ensure the correction of a suitable number of epidermal stem cells, responsible for the long-term restoration of the genetic defect. In addition, despite the high VCN obtained in SIN-transduced samples (VCN=11), the expression level of the therapeutic protein resulted to be from 3 to 9 times lower with respect to the wild-type sample (which has 2 copies/alleles of the *COL17A1* gene). By contrast, data obtained with the γRV-*COL17A1* vector resulted to be very promising in both the transduction efficiency and the expression of the therapeutic protein with a VCN of 3 and, hence, with a limited impact on the genome of the target keratinocytes.

Experiments comparing the (i) SIN-γRV-*COL17A1*, (ii) SIN-γRV-*COL7A1* and (iii) γRV-*COL17A1* vectors shed light on important expression issues exclusively related to the *COL17A1* transgene in a SIN-γRV asset. These expression issues are caused, in the first place, by the presence of rearrangements of the integrated cassette that involve not only the *COL17A1* transgene but also the external viral backbone.

Secondly, analysis of *COL17A1* transcripts showed an elevated number of alternative transcripts in the SIN-γRV-transduced samples as compared with the γRV-transduced samples or, even more, the wild-type cells. This suggests that the EF1α promoter may affect the splicing pattern of the *COL17A1* differently from the LTR and the endogenous *COL17A1* promoter. Splicing and transcription are deeply intertwined and both processes can affect each other [70].

Bioinformatic analysis of the splicing sites revealed the presence of strong splicing donor/acceptor pairs that could be accountable for the alternative transcripts in SIN-γRV-transduced cultures. Although, more data are necessary for a full understanding of this phenomenon and to verify a possible instability of the mRNA generated in SIN-γRV-transduced samples.

To conclude, here we demonstrate that the γRV-*COL17A1* seems to be the only vector suitable for a combined cell and gene therapy approach for *COL17A1*-dependent JEB.

About the safety concerns raised by insertional genotoxicity events in the hematopoietic tissue [59, 60, 68, 71-75], genotoxic events encountered in γRV-based gene therapy products suggest that insertional oncogenesis could be related to cell type, patient's genetic background, specific disease, age, transgene, or other mutations (Fig.18, upper panel) [64]. In the skin, γRV has already been used for the *LAMB3*-dependent JEB and *COL7A1*-dependent RDEB and no adverse event due to the vector integration was observed even with a long-term follow-up [54, 57, 61, 63].

Studies focusing on the integration pattern of the γRV and the SIN-γRV are currently being carried out by our group. Preliminary data show that there is no difference in the genomic regions targeted by these two different vectors and no perturbation of proto-oncogenes is observed (Fig. 18, lower

panel).

Disease	Trial Number (Phase)	Starting Year; Site	Vector	No. of Pt	SAEs	Deaths	Age of SAEs	IS Clusters
SCID-X1	N/A	1999; France	γRV-IL-2Rγ	10	5 (50%)	1	2.5–5.5 yr	*LMO2*, *BMI1v* and *CCND2*
	N/A	2002; UK	γRV-IL-2Rγ	10	1 (10%)	0		
WAS	DRKS00000330 (phase I/II)	2006; Germany	γRV-WAS	10	9 (90%)	3	1.5–5 yr	*LMO2*, *MDS1*, and *MN1*
ADA-SCID	NCT00599781 (phase I/II)	2000; Italy	γRV-ADA	12	0	0		
	NCT03478670 (phase IV)	2017; Italy	γRV-ADA	6	0*	0		
	NCT00018018 (phase I/II)	2001; US	γRV-ADA	10	0	0		
	NCT00794508 (phase II)	2009; US	γRV-ADA	10	0	0		
	NCT01279720 (phase I/II)	2003; UK	γRV-ADA	8	0	0		
CGD	NCT00564759 (phase I/II)	2004; Germany	γRV-CYBB	2	2 (100%)	1	2 yr	*MECOM*, *PRDM16*, and *SETBP1*
	NCT00927134 (phase I/II)	2004; Switzerland	γRV-CYBB	1	1 (100%)	1		
RDEB	NCT01263379 (Phase I/II)	2010; US	γRV-COL7A1	7	0	0		
JEB	N/A	2005; Italy, 2014; Austria, 2015; Germany	γRV-LAMB3	3	0	0		

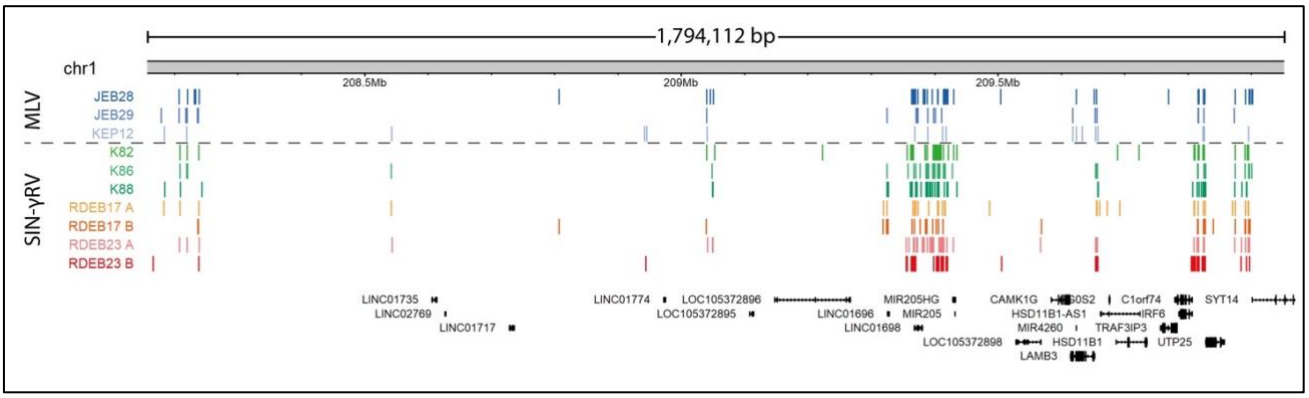

Figure 18. Comparison of the γRV and the SIN-γRV integration pattern. Upper panel: list of genotoxic events in γRV-based gene therapy studies [64]. Lower panel: an example of the integration pattern observed in samples transduced with γRV vector (in blue) or with SIN-γRV vector (in green and red). Chromosome 1 integrations are depicted (unpublished data).

This work elucidates the complexity of the development of a therapeutic approach for *COL17A1*-JEB. Despite the success of its "brother" SIN-γRV-*COL7A1*, the use of a SIN-γRV-*COL17A1* in this project highlighted *COL17A1*-related expression issues and its inadequacy as a therapeutic option.

Throughout my doctorate, many efforts were done to implement the use of SIN-γRV-*COL17A1* and to understand the reasons for the low transgene expression, although some queries remain unsolved. To achieve Collagen 17 expression comparable to a healthy donor, a faster and more reliable approach may be to maintain the use of the MLV-derived γRV as demonstrated in this work.

An alternative strategy is also possible. Given its role in regulating some aspects of epidermal stem cells [76-78], *COL17A1* seems to require a physiological regulation of its expression and some regulatory elements are harbored internally to the gene. In this light, a homology-directed repair (HDR) approach may be suitable for such a gene. Recently, a group demonstrated the possibility to modify large portions of specific genomic DNA using single-stranded DNA (ssDNA) HDR templates (HDRTs) that boost knock-in efficiency [79]. The combination of this approach with the use of small

molecules that enhance HDR has been shown to increase knock-in efficiencies in hematopoietic cells [80]. This approach could be also applied to *COL17A1*, and primary keratinocytes [79, 81]. Mutations in the exons 41-53 of *COL17A1* seem to cause the most severe phenotypes, and a precise substitution of this region could be reached by employing the strategy described above. This may pave the way for the establishment of a unique gene editing strategy for the most severe *COL17A1* phenotypes. This approach represents an alternative strategy to tackle recessive forms, but there is still a long way to go. It could be a unique chance to maintain a physiological expression of COL17 and obtain a permanent stem cell correction.

5 MATERIAL AND METHODS

5.1 Cell culture and maintenance

3T3-J2 cell line. Mouse 3T3-J2 cells were a gift from H. Green, Harvard Medical School. 3T3-J2 cells were cultured in Dulbecco's modified Eagle's medium (DMEM) supplemented with 10% irradiated calf serum, glutamine (4 mM), and penicillin-streptomycin (50 IU/ml).

Human primary keratinocytes. Human primary keratinocytes were retrieved from biopsies of healthy adult donors. A skin biopsy was minced and trypsinized (0.05% trypsin and 0.01% EDTA) at 36,5°C for 3h. Keratinocytes were collected every 30 minutes, plated (2,7 x 10^4 cells per cm^2) onto lethally irradiated 3T3-J2 cells (2,7 x 10^4 cells per cm^2) and allowed to grow at 36,5°C with 5% CO2 and humidified atmosphere. Cells were grown in KNO medium (DMEM (60%), Ham's F12 nutrient mixture (30%), irradiated fetal bovine serum (FBS) (10%), penicillin-streptomycin (50 IU/ml), glutamine (4 mM), adenine (0.18 mM), insulin (5 μg/ml), hydrocortisone (0.4 μg/ml), cholera toxin (0.1 nM), triiodothyronine (2 nM)). After 3 days, the KNO medium was replaced with the KC medium (KNO medium containing EGF (10 ng/ml)). After reaching sub-confluence, keratinocytes were trypsinized (0.05% trypsin and 0.01% EDTA) at 36,5°C for 15-20 min and replated (6 x 10^3 cells per cm^2) onto a new feeder layer (2,7 x 10^4 cells per cm^2) in KNO medium, swapped with KC after 3 days. Sub-confluent cultures were frozen in liquid nitrogen (1 x 10^6 cells per vial).

GABEB cells. Generalized atrophic benign epidermolysis bullosa (GABEB) cells were cultured in EpiLife medium (Gibco) supplemented with Human Keratinocytes Growth Factor (HKGF) supplement (Gibco) at 36,5°C with 5% CO2 and humidified atmosphere. At sub-confluence, GABEB cells were trypsinized (0.05% trypsin and 0.01% EDTA) at 36,5°C for 10 min, diluted 1:3-1:5, and plated in fresh medium. Change of the medium was performed every other day.

HeLa cells. Immortalized HeLa cells were cultured in DMEM supplemented with 10% heat-inactivated fetal bovine serum, glutamine (2mM), and penicillin-streptomycin (100 IU/ml) medium

at 36,5°C with 5% CO2 and humidified atmosphere. At sub-confluence, HeLa cells were trypsinized (0.05% trypsin and 0.01% EDTA) at 36,5°C for 5 min, diluted 1:5-1:10, and plated in fresh medium.

FREEZING PROCEDURE

Human primary keratinocytes. Sub-confluent keratinocytes cell cultures were trypsinized and resuspended in a KNO medium supplemented with 10% glycerol. Collected keratinocytes were aliquoted and frozen at -80°C. 24h later, cells were relocated in liquid nitrogen for long-term storage.
GABEB and HeLa cells. Sub-confluent cell cultures were trypsinized and resuspended in FBS supplemented with 10% DMSO. Collected cells were aliquoted and frozen at -80°C. 24h later, cells were relocated in liquid nitrogen for long-term storage.

THAWING PROCEDURE

Human primary keratinocytes. A vial of frozen cells (KEP15, KEP19, and NHK cells) was transferred from liquid nitrogen storage onto dry ice.
The cell vial was thawed slowly in the water bath at 37°C until only a small sphere of frozen volume remained. The thawed cells were transferred into a 15ml tube with fresh warmed-up KNO medium and centrifuged at 1400g for 5 minutes at room temperature. The cell pellet was resuspended in fresh KNO medium, plated (6 x 10^3 cells per cm^2) onto lethally irradiated 3T3-J2 cells (2,7 x 10^4 cells per cm^2), and allowed to grow at 36,5°C with 5% CO2 and humidified atmosphere.
GABEB and HeLa cells. A vial of frozen cells was transferred from liquid nitrogen storage onto dry ice.
The cell vial was thawed slowly in the water bath at 37°C until only a small sphere of frozen volume remained. The thawed cells were transferred into a 15ml tube with fresh warmed-up medium and centrifuged at 240g for 5 minutes at room temperature. The cell pellet was resuspended in fresh medium, plated 3 x 10^4 cells per cm^2, and allow to grow at 36,5°C with 5% CO2 and humidified atmosphere.

5.2 Transduction process

Human primary keratinocytes (supernatant-based method). Keratinocyte cells (KEP15 and KEP19) were thawed and plated (6 x 10^3 cells per cm^2) onto lethally irradiated 3T3-J2 cells (2,7 x 10^4 cells per cm^2) in KNO medium until sub-confluence was reached. Sub-confluent keratinocytes were trypsinized and transduced at MOI10 (adjusted for the 3T3-J2 cell that will seize part of the viral supernatant) as follows:

- non-tissue treated plates were coated by using 5 μg / cm^2 of RetroNectin (Takara) diluted in dPBS and allowed to deposit overnight at 4°C.
- the day after, RetroNectin was removed, and the dish was washed with PBS1X once.
- SIN-γRVs were diluted in KNO medium according to the desired MOI and carefully added to the RetroNectin-coated dish.
- the virus was allowed to deposit for 4 hours at 36,5°C with 5% CO2 in a humidified atmosphere.
- after 4 hours viral supernatant was eliminated and keratinocytes and irradiated 3T3-J2 cells were plated.

Human primary keratinocytes (co-culture method). Sub-confluent primary cultures were trypsinized and seeded ($6x10^3$ cells per cm^2) onto a feeder layer ($2,7\ x10^4$ cells per cm^2) composed of lethally irradiated 3T3-J2 cells and producer AM12-*COL17A1* cells (a 1:2 mixture) in KNO medium. After 3 days of cultivation, keratinocytes were collected and replated on a regular 3T3-J2 feeder layer.

GABEB cells. The transduction procedure of GABEB cells was performed using RetroNectin as a transduction enhancer. The process occurred as follows:

- non-tissue treated plates were coated by using 5 μg / cm^2 of RetroNectin (Takara) diluted in dPBS and allowed to deposit overnight at 4°C.
- the day after, RetroNectin was removed, and the dish was carefully washed with PBS1X once.
- SIN-γRVs was diluted in EpiLife supplemented with HKGF medium according to the desired MOI and carefully added to the RetroNectin-coated dish.
- the virus was allowed to deposit for 4 hours at 36,5°C with 5% CO2 in a humidified atmosphere.
- after 4 hours viral supernatant was eliminated and GABEB cells were plated $1x10^4$cell/cm^2

5.3 Immunofluorescent staining

For immunofluorescence analyses of in vitro cultured keratinocytes, cells were plated onto glass coverslips ($1x10^3$ keratinocytes/$cm^{2)}$ and grown as previously described. Cells were fixed with PFA 3% for 10 min at room temperature, carefully washed with 1X PBS, and permeabilized in PBS/Triton 0.2% for 20 min. Blocking solution (FBS 5% BSA 2% in PBS/Triton 0.1%) was added for 30 min at 37°C. Primary antibodies were diluted in a Blocking solution as described in Table 5.1 and added to the samples for 2 hours at 37°C after blocking. Secondary antibodies were diluted in blocking solution

as described in Table 5.1 and added to the samples for 30 min at 37°C. Cell nuclei were stained with DAPI. Dako Mounting medium was used to mount coverslips. Zeiss Axio Imager. A1 was used to visualize fluorescent signals.

Table 5.1 List of antibodies used to perform the immunofluorescence assays.

Antibody	Catalog number	Supplier	Dilution	Specie
anti-COL17	ab184996	Abcam	1:2000	rabbit
Anti-COL7	Sc-53226	Santa Cruz Biotechnology	1:500	mouse
Anti pankeratin	MA5-13203	Invitrogen	1:500	mouse
Anti pankeratin	Ab9377	Abcam	1:1000	rabbit
anti-Mouse IgG (H+L) Alexa Fluor 568	A10037	Thermo Fisher Scientific	1:1000	donkey
anti-Rabbit IgG (H+L) Alexa Fluor 488	A21206	Thermo Fisher Scientific	1:1000	donkey

5.4 Provirus vector copy number (VCN) evaluation

Vector copy number analysis was performed on the genomic DNA of transduced cells.

Genomic DNA was isolated from pellets of cells with QIAmp DNA Mini Kit (Qiagen) following the manufacturer's instructions.

A transduced cell clone was used as a reference for VCN evaluation. Its VCN was assessed to be 1 via Southern blot analysis and confirmed by sequencing.

TaqMan Universal PCR Master Mix and *COL17A1*, *COL7A1* cDNA, and genomic GAPDH were used to perform the real-time PCR reaction. Reactions were performed with ABI Prism 7900 Sequence Detection System (Applied Biosystems), using 10 ng genomic DNA. The relative quantity that relates to the PCR signal of the target gene was normalized to the level of GAPDH (internal control gene) in the same genomic DNA by using the $2^{-\Delta\Delta Ct}$ quantification).

Table 5.2 List of TaqMan® probes used for qRT-PCR.

Target	Catalog number
GAPDH (genomic)	Hs03929097_g1
COL17A1 (cDNA)	Hs00990073_m1
COL7A1 (cDNA)	HS00164310_m1

5.5 Protein extraction and western blot analysis

Cell pellets for western analysis were lysed in RIPA buffer (Sigma Aldrich) supplemented with Phosphatase and Protease Inhibitor Cocktail (Thermo Fisher) for 30' on ice. The samples were then centrifuged for 20 minutes at 14000 rpm at 4°C and the supernatant was collected and stored at -80°C.

For the analysis of secreted proteins (collagen 7 and the extracellular domain of collagen 17), cells were starved with KC medium without FBS for 48 hours. Then, the conditioned medium was collected, filtered through 0.22-μm pore cellulose acetate filters, and concentrated with Amicon Ultra Centrifugal filter 10k (Merk Millipore).

BCA kits (Pierce) were used to quantify the total protein amount. The same quantity of proteins was loaded in 4–12% NuPAGE Bis-Tris Gels or 3-8% NuPage Tris-Acetate Gels (Thermo Fisher) at 100 V for 2 h and transferred 100 V at 4°C for 2 h onto nitrocellulose membrane (Millipore). Membranes were treated with Blotting-Grade Blocker (Bio-Rad) for 1h at room temperature. Primary antibodies were diluted in blocking buffer as indicated in Table 5.3, added to the membranes, and incubated overnight at 4 °C. Secondary antibodies were diluted in blocking buffer as indicated in Table 5.3 and added to the corresponding membranes for 1h at room temperature. The signal was visualized with Clarity Western ECL substrate (Bio-Rad) using ChemiDoc (Bio-Rad). Bio-Rad's Image Lab software 6.0 was used for band densitometry.

Table 5.3 List of antibodies used in Western Blot analysis.

Antibody	Catalog number	Supplier	Dilution	Specie
anti-COL17	ab184996	Abcam	1:1000	rabbit
Anti-COL7	Sc-53226	Santa Cruz Biotechnology	1:500	mouse
anti-GAPDH	ab8245	Abcam	1:10000	mouse
Anti-beta Actin	Ab3280	Abcam	1:5000	mouse
Anti-Vinculin	V4505	Sigma	1:10000	mouse
anti-rabbit IgG HRP	sc-2313	Santa Cruz Biotechnology	1:5000	donkey
anti-mouse IgG HRP	sc-2314	Santa Cruz Biotechnology	1:5000-1:10000	donkey

5.6 Expression cassette integrity analysis

Viral cassette integrity analysis was performed on the genomic DNA of transduced clones.

Genomic DNA was extracted from clones using the QIAamp® DNA Mini Kit and amplified with specific primers for the expression cassette. The amplified fragments were resolved on 1% agarose gel. Due to the extension of the expression cassette (approximately 5.3 kb), three primer pairs were used for the amplification (table 5.4).

Table 5.4 Primers used to amplify the *COL17A1* expression cassette.

	Primer Fw	Primer Rev	Expected size
PCR 1	5'GAGCGCACATCGCCCACAG 3'	5'CCAGAGCAATGAGGCCGAAG 3'	1800bp
PCR 2	5'GGCAAGACCACCACTGCAG 3'	5'TTGGTGTCCTCTGGGGCCTG 3'	1539bp
PCR 3	5'GGATCGTTCCTGTCCAACTC 3'	5'CAGGAAGATGTCGACGTCAGC 3'	2325bp

5.7 Splicing analysis

Total RNA was extracted from the pellets of primary human keratinocytes using the PureLink RNA Mini Kit (Thermo Fisher) according to the manufacturer's instructions. Complementary DNA was generated using the SuperScript VILO cDNA Synthesis Kit (Thermo Fisher).

TaKaRa LA Taq polymerase (TaKaRa) was used to amplify the entire *COL17A1* coding sequence starting from 30 ng of the retrotranscribed cDNA. The following primers were used:

- Primer Forward 5' CTAGAAGAAAACATCAGGAGGAG 3'
- Primer Reverse 5' CTAGCTCACGGCTTGACAGC 3'

PCR conditions are reported in table 5.5.

Table 5.5 Thermocycler settings for PCR reaction.

95°C	2 min	
95°C	30 sec	33 cycles
65°C	30 sec	
68°C	5 min	
72°C	7 min	

The PCR products were analyzed on 0,8% agarose gel (Sigma).

5.8 Plasmid construct

Cloning process of *COL17A1* for stable packaging cell line establishment. *COL17A1* cDNA sequence (4494bp), along with its 5' UTR sequence, was cloned into the pbib-ETAR-fcvi-ES-12-6(g)ps, an exchange vector designed by BioNTech IMFS, resulting in the pbib-*COL17A1* construct. The expression is driven by the Elongation Factor 1a short promoter (212bp) and the woodchuck

hepatitis virus post-transcriptional regulatory element (WPRE) was placed downstream of the gene to increase COL17 expression.

Cloning process of *COL17A1* for transient virus production. The cloning strategy of the K14-*COL17A1* SIN-γRV consisted of the isolation of *COL17A1* cDNA sequence, along with its 5' UTR sequence, from the pbib-*COL17A1* vector followed by the cloning step into a pSRS-SIN-γRV, already containing the human K14 promoter. The resulting pSRS-K14-*COL17A1* construct was checked by diagnostic digestion and Sanger sequencing (Eurofins Genomics).

As for the EF1α-*COL17A1* construct, the entire expression cassette (made of EF1α promoter, 5' UTR, *COL17A1* open reading frame, and WPRE sequence) was isolated and transferred to the pSRS-SIN γ retroviral vector deprived of the K14 promoter. The resulting pSRS-EF1α-*COL17A1* construct was checked by diagnostic digestion and Sanger sequencing (Eurofins Genomics).

The γRV-*COL17A1* was already present in house.

5.9 Viral production

Stable viral production. Stable viral production was performed by BioNTech according to their well-established protocol. Pbib-*COL17A1* construct and 293Vec-AMPHO® cells were used as starting material.

Titration was performed on HeLa cells and monitored by flow cytometry. The typical viral titer was 5-6 x 10^6 UI/ml.

Transient viral production. Phoenix-AMPHO cells were cultured in DMEM supplemented with 10% heat-inactivated non-irradiated Fetal Bovine Serum, 1% Glutamine, and 1% penicillin-streptomycin antibiotics (Gibco). Fresh DNA of each transfer vector was used for the transient transfection of Phoenix-AMPHO cells with calcium phosphate for retroviral production. Transfection efficiencies were monitored by immunofluorescence.

Infectious retroviruses were harvested for 48 hours post-transfection, filtered through 0.45-μm pore cellulose acetate filters, and concentrated by ultracentrifugation (17,000g at 4°C for 16 hours). The final viral pellets were resuspended in PBS-BSA 1% in ice and aliquots of viral stocks were kept at −80°C until further use. The viral titer was assessed on GABEB cells by immunofluorescence. The typical viral titer was 1-2 x 10^5 UI/ml.

5.10 Clean-up evaluation

The successful clean-up process was monitored through the PCR amplification of the neomycin resistance gene using genomic DNA as a template and universal oligos for the inserted pbib-

COL17A1 vector (5'-oligo) and the genomic locus (3'-oligo) of 293Vec-AMPHO cells. The PCR fragment of the clean-up reaction was confirmed by sequencing.

Table 5.6 Primers used to amplify the neomycin gene.

	Sequence
5'- oligo	5' TCCAGGCTCTAGTTTTGAC 3'
3'- oligo	5' CCCATGCGTTGATTCATGC 3'

5.11 FACS staining protocol for viral titration

Determination of the viral titer was performed via antibody stain and the subsequent flow cytometric analysis on HeLa cells. To perform the cell staining, Fix & Perm kit (Thermo Fisher) and the antibodies outlined in table 5.7 were used.

Table 5.7 List of antibodies used to perform the FACS assay.

Antibody	Catalog number	Supplier	Dilution	Specie
anti-COL17	ab184996	Abcam	1:25	rabbit
Anti-rabbit igG-FITC	F1262	Sigma	1:25	goat

One million trypsinized HeLa cells were washed with PBS1X-FBS 2%-EDTA 2mM, centrifuged at 300g for 5 minutes, and resuspended in 100ul of the fixation solution (Solution A). The samples were allowed to incubate for 15 min at RT in the dark. The reaction was stopped by adding 2 ml of PBS1X-FBS 2%-EDTA 2mM and centrifuging the samples for 5 min at 300g at RT. 100ul permeabilization solution B was, then, added and the pellets were carefully resuspended. 20 ul of diluted primary antibody were added and allowed to incubate for 20 min at RT in the dark. The reaction was stopped by adding 2 ml of PBS1X-FBS 2%-EDTA 2mM and centrifuging the samples for 5 min at 300g at RT. 100ul permeabilization solution B was added and the pellets were carefully resuspended. 20 ul of diluted secondary antibody were added and allowed to incubate for 20 min at RT in the dark. The reaction was stopped by adding 2ml of PBS1X-FBS 2%-EDTA 2mM and centrifuging the samples for 5 min at 300g at RT. An additional wash was performed with PBS1X-FBS 2%-EDTA 2mM buffer. To proceed with the analysis with the flow cytometer, cells were resuspended in 1 ml of PBS1X-FBS 2%-EDTA 2mM and processed within the next two hours.

HeLa cells were analyzed by flow cytometry (BD FACSCanto II), and data were collected using BD FACSDiva Software v6.1.3.

6 REFERENCES

1. Yousef, H., M. Alhajj, and S. Sharma, *Anatomy, Skin (Integument), Epidermis*, in *StatPearls*. 2022: Treasure Island (FL).
2. *Chu DH. 2008. Chapter 7. Development and Structure of Skin. in Fitzpatrick'sDermatology in General Medicine, e.e.L.G., K Wolff, SI Katz, BAGilchrest, AS Paller, DJ Leffell). The McGraw-Hill Companies, New York, NY.*
3. Watt, F.M., *The stem cell compartment in human interfollicular epidermis.* J Dermatol Sci, 2002. **28**(3): p. 173-80.
4. Gambardella, L. and Y. Barrandon, *The multifaceted adult epidermal stem cell.* Curr Opin Cell Biol, 2003. **15**(6): p. 771-7.
5. Blanpain, C. and E. Fuchs, *Epidermal stem cells of the skin.* Annu Rev Cell Dev Biol, 2006. **22**: p. 339-73.
6. Fuchs, E., *Scratching the surface of skin development.* Nature, 2007. **445**(7130): p. 834-42.
7. Blanpain, C. and E. Fuchs, *Stem cell plasticity. Plasticity of epithelial stem cells in tissue regeneration.* Science, 2014. **344**(6189): p. 1242281.
8. Nievers, M.G., R.Q. Schaapveld, and A. Sonnenberg, *Biology and function of hemidesmosomes.* Matrix Biol, 1999. **18**(1): p. 5-17.
9. Walko, G., M.J. Castañón, and G. Wiche, *Molecular architecture and function of the hemidesmosome.* Cell Tissue Res, 2015. **360**(3): p. 529-44.
10. Hieda, Y., et al., *Identification of a new hemidesmosomal protein, HD1: a major, high molecular mass component of isolated hemidesmosomes.* J Cell Biol, 1992. **116**(6): p. 1497-506.
11. Owaribe, K., et al., *The hemidesmosomal plaque. I. Characterization of a major constituent protein as a differentiation marker for certain forms of epithelia.* Differentiation, 1990. **45**(3): p. 207-20.
12. Fontao, L., et al., *Regulation of the type II hemidesmosomal plaque assembly in intestinal epithelial cells.* Exp Cell Res, 1999. **250**(2): p. 298-312.
13. Uematsu, J., et al., *Demonstration of type II hemidesmosomes in a mammary gland epithelial cell line, BMGE-H.* J Biochem, 1994. **115**(3): p. 469-76.
14. Kelly, D.E., *Fine structure of desmosomes. , hemidesmosomes, and an adepidermal globular layer in developing newt epidermis.* J Cell Biol, 1966. **28**(1): p. 51-72.
15. Tidman, M.J. and R.A. Eady, *Ultrastructural morphometry of normal human dermal-epidermal junction. The influence of age, sex, and body region on laminar and nonlaminar components.* J Invest Dermatol, 1984. **83**(6): p. 448-53.
16. Tidman, M.J. and R.A. Eady, *Hemidesmosome heterogeneity in junctional epidermolysis bullosa revealed by morphometric analysis.* J Invest Dermatol, 1986. **86**(1): p. 51-6.
17. Rezniczek, G.A., et al., *Linking integrin alpha6beta4-based cell adhesion to the intermediate filament cytoskeleton: direct interaction between the beta4 subunit and plectin at multiple molecular sites.* J Cell Biol, 1998. **141**(1): p. 209-25.
18. Litjens, S.H., J.M. de Pereda, and A. Sonnenberg, *Current insights into the formation and breakdown of hemidesmosomes.* Trends Cell Biol, 2006. **16**(7): p. 376-83.
19. Walko, G., et al., *Targeted proteolysis of plectin isoform 1a accounts for hemidesmosome dysfunction in mice mimicking the dominant skin blistering disease EBS-Ogna.* PLoS Genet, 2011. **7**(12): p. e1002396.
20. Fine, J.D., et al., *The classification of inherited epidermolysis bullosa (EB): Report of the Third International Consensus Meeting on Diagnosis and Classification of EB.* J Am Acad Dermatol, 2008. **58**(6): p. 931-50.
21. Fine, J.D., et al., *Cause-specific risks of childhood death in inherited epidermolysis bullosa.* J Pediatr, 2008. **152**(2): p. 276-80.

22. Yuen, W.Y. and M.F. Jonkman, *Risk of squamous cell carcinoma in junctional epidermolysis bullosa, non-Herlitz type: report of 7 cases and a review of the literature.* J Am Acad Dermatol, 2011. **65**(4): p. 780-789.
23. Mallipeddi, R., et al., *Increased risk of squamous cell carcinoma in junctional epidermolysis bullosa.* J Eur Acad Dermatol Venereol, 2004. **18**(5): p. 521-6.
24. Bardhan, A., et al., *Epidermolysis bullosa.* Nat Rev Dis Primers, 2020. **6**(1): p. 78.
25. Varki, R., et al., *Epidermolysis bullosa. I. Molecular genetics of the junctional and hemidesmosomal variants.* J Med Genet, 2006. **43**(8): p. 641-52.
26. Has, C., et al., *Consensus reclassification of inherited epidermolysis bullosa and other disorders with skin fragility.* Br J Dermatol, 2020. **183**(4): p. 614-627.
27. Fine, J.D., *Inherited epidermolysis bullosa.* Orphanet J Rare Dis, 2010. **5**: p. 12.
28. Yuen, W.Y., et al., *Long-term follow-up of patients with Herlitz-type junctional epidermolysis bullosa.* Br J Dermatol, 2012. **167**(2): p. 374-82.
29. Abu Sa'd, J., et al., *Molecular epidemiology of hereditary epidermolysis bullosa in a Middle Eastern population.* J Invest Dermatol, 2006. **126**(4): p. 777-81.
30. Gatalica, B., et al., *Cloning of the human type XVII collagen gene (COL17A1), and detection of novel mutations in generalized atrophic benign epidermolysis bullosa.* Am J Hum Genet, 1997. **60**(2): p. 352-65.
31. Natsuga, K., et al., *Life before and beyond blistering: The role of collagen XVII in epidermal physiology.* Exp Dermatol, 2019. **28**(10): p. 1135-1141.
32. Areida, S.K., et al., *Properties of the collagen type XVII ectodomain. Evidence for n- to c-terminal triple helix folding.* J Biol Chem, 2001. **276**(2): p. 1594-601.
33. Schäcke, H., et al., *Two forms of collagen XVII in keratinocytes. A full-length transmembrane protein and a soluble ectodomain.* J Biol Chem, 1998. **273**(40): p. 25937-43.
34. Franzke, C.W., et al., *Transmembrane collagen XVII, an epithelial adhesion protein, is shed from the cell surface by ADAMs.* Embo j, 2002. **21**(19): p. 5026-35.
35. Hirako, Y., et al., *Cleavage of BP180, a 180-kDa bullous pemphigoid antigen, yields a 120-kDa collagenous extracellular polypeptide.* J Biol Chem, 1998. **273**(16): p. 9711-7.
36. Hirako, Y., et al., *The 97-kDa (LABD97) and 120-kDa (LAD-1) fragments of bullous pemphigoid antigen 180/type XVII collagen have different N-termini*, in *J Invest Dermatol*. 2003: United States. p. 1554-6.
37. Nishie, W., et al., *Ectodomain shedding generates Neoepitopes on collagen XVII, the major autoantigen for bullous pemphigoid.* J Immunol, 2010. **185**(8): p. 4938-47.
38. Condrat, I., et al., *Junctional Epidermolysis Bullosa: Allelic Heterogeneity and Mutation Stratification for Precision Medicine.* Front Med (Lausanne), 2018. **5**: p. 363.
39. Schmidt, E., et al., *Localisation of bullous pemphigoid antigen 180 (BP180) in cultured human keratinocytes: functionally relevant modification by calcium.* Arch Dermatol Res, 2006. **298**(6): p. 283-90.
40. Amber, K.T., et al., *Autoimmune Subepidermal Bullous Diseases of the Skin and Mucosae: Clinical Features, Diagnosis, and Management.* Clin Rev Allergy Immunol, 2018. **54**(1): p. 26-51.
41. ORPHANET, *Intermediate Generalized Junctional Epidermolysis Bullosa*.
42. Bauer, J.W. and C. Lanschuetzer, *Type XVII collagen gene mutations in junctional epidermolysis bullosa and prospects for gene therapy.* Clin Exp Dermatol, 2003. **28**(1): p. 53-60.
43. Mohammed Qumani Ahmed, F.S.H.A., S. M. A. Shahid and Mohd Adnan Kausar, *Molecular Structure and Function of the Hemidesmosome: New Insights and Advances*.
44. Cogan, J., et al., *Aminoglycosides restore full-length type VII collagen by overcoming premature termination codons: therapeutic implications for dystrophic epidermolysis bullosa.* Mol Ther, 2014. **22**(10): p. 1741-52.

45. Lincoln, V., et al., *Gentamicin induces LAMB3 nonsense mutation readthrough and restores functional laminin 332 in junctional epidermolysis bullosa.* Proc Natl Acad Sci U S A, 2018. **115**(28): p. E6536-e6545.
46. Atanasova, V.S., et al., *Amlexanox Enhances Premature Termination Codon Read-Through in COL7A1 and Expression of Full Length Type VII Collagen: Potential Therapy for Recessive Dystrophic Epidermolysis Bullosa.* J Invest Dermatol, 2017. **137**(9): p. 1842-1849.
47. Has, C., et al., *Read-Through for Nonsense Mutations in Type XVII Collagen–Deficient Junctional Epidermolysis Bullosa.* J Invest Dermatol, 2022. **142**(4): p. 1227-1230.e4.
48. Li, Y., et al., *Gentamicin induces COL17A1 nonsense mutation readthrough in junctional epidermolysis bullosa.* J Dermatol, 2020. **47**(3): p. e82-e83.
49. Woodley, D.T., et al., *Gentamicin induces functional type VII collagen in recessive dystrophic epidermolysis bullosa patients.* J Clin Invest, 2017. **127**(8): p. 3028-3038.
50. Prodinger, C., et al., *Epidermolysis bullosa: Advances in research and treatment.* Exp Dermatol, 2019. **28**(10): p. 1176-1189.
51. Jacków, J., et al., *Collagen XVII Shedding Suppresses Re-Epithelialization by Directing Keratinocyte Migration and Dampening mTOR Signaling.* J Invest Dermatol, 2016. **136**(5): p. 1031-1041.
52. Pellegrini, G., et al., *The control of epidermal stem cells (holoclones) in the treatment of massive full-thickness burns with autologous keratinocytes cultured on fibrin.* Transplantation, 1999. **68**(6): p. 868-79.
53. Pellegrini, G., et al., *Long-term restoration of damaged corneal surfaces with autologous cultivated corneal epithelium.* Lancet, 1997. **349**(9057): p. 990-3.
54. Hirsch, T., et al., *Regeneration of the entire human epidermis using transgenic stem cells.* Nature, 2017. **551**(7680): p. 327-332.
55. De Luca, M., G. Pellegrini, and H. Green, *Regeneration of squamous epithelia from stem cells of cultured grafts.* Regen Med, 2006. **1**(1): p. 45-57.
56. Pellegrini, G., et al., *Epithelial stem cells in corneal regeneration and epidermal gene therapy.* J Pathol, 2009. **217**(2): p. 217-28.
57. Mavilio, F., et al., *Correction of junctional epidermolysis bullosa by transplantation of genetically modified epidermal stem cells.* Nat Med, 2006. **12**(12): p. 1397-402.
58. Siprashvili, Z., et al., *Safety and Wound Outcomes Following Genetically Corrected Autologous Epidermal Grafts in Patients With Recessive Dystrophic Epidermolysis Bullosa.* JAMA, 2016. **316**(17): p. 1808-1817.
59. Howe, S.J., et al., *Insertional mutagenesis combined with acquired somatic mutations causes leukemogenesis following gene therapy of SCID-X1 patients.* J Clin Invest, 2008. **118**(9): p. 3143-50.
60. Hacein-Bey-Abina, S., et al., *Insertional oncogenesis in 4 patients after retrovirus-mediated gene therapy of SCID-X1.* J Clin Invest, 2008. **118**(9): p. 3132-42.
61. Montini, E., et al., *The genotoxic potential of retroviral vectors is strongly modulated by vector design and integration site selection in a mouse model of HSC gene therapy.* J Clin Invest, 2009. **119**(4): p. 964-75.
62. Eichstadt, S., et al., *Phase 1/2a clinical trial of gene-corrected autologous cell therapy for recessive dystrophic epidermolysis bullosa.* JCI Insight, 2019. **4**(19).
63. So, J.Y., et al., *Long-term safety and efficacy of gene-corrected autologous keratinocyte grafts for recessive dystrophic epidermolysis bullosa.* Orphanet J Rare Dis, 2022. **17**(1): p. 377.
64. Palamenghi, M., M. De Luca, and L. De Rosa, *The steep uphill path leading to ex vivo gene therapy for genodermatoses.* Am J Physiol Cell Physiol, 2022. **323**(3): p. C896-c906.
65. Kueckelhaus, M., et al., *Transgenic Epidermal Cultures for Junctional Epidermolysis Bullosa - 5-Year Outcomes.* N Engl J Med, 2021. **385**(24): p. 2264-2270.

66. Zychlinski, D., et al., *Physiological promoters reduce the genotoxic risk of integrating gene vectors.* Mol Ther, 2008. **16**(4): p. 718-25.
67. Avedillo Díez, I., et al., *Development of novel efficient SIN vectors with improved safety features for Wiskott-Aldrich syndrome stem cell based gene therapy.* Mol Pharm, 2011. **8**(5): p. 1525-37.
68. Thornhill, S.I., et al., *Self-inactivating gammaretroviral vectors for gene therapy of X-linked severe combined immunodeficiency.* Mol Ther, 2008. **16**(3): p. 590-8.
69. Hennig, K., et al., *HEK293-based production platform for γ-retroviral (self-inactivating) vectors: application for safe and efficient transfer of COL7A1 cDNA.* Hum Gene Ther Clin Dev, 2014. **25**(4): p. 218-28.
70. Kolathur, K.K., *Role of promoters in regulating alternative splicing.* Gene, 2021. **782**: p. 145523.
71. Stein, S., et al., *Genomic instability and myelodysplasia with monosomy 7 consequent to EVI1 activation after gene therapy for chronic granulomatous disease.* Nat Med, 2010. **16**(2): p. 198-204.
72. Ott, M.G., et al., *Correction of X-linked chronic granulomatous disease by gene therapy, augmented by insertional activation of MDS1-EVI1, PRDM16 or SETBP1.* Nat Med, 2006. **12**(4): p. 401-9.
73. Braun, C.J., et al., *Gene therapy for Wiskott-Aldrich syndrome--long-term efficacy and genotoxicity.* Sci Transl Med, 2014. **6**(227): p. 227ra33.
74. Hacein-Bey-Abina, S., et al., *A serious adverse event after successful gene therapy for X-linked severe combined immunodeficiency*, in *N Engl J Med*. 2003: United States. p. 255-6.
75. Hacein-Bey-Abina, S., et al., *LMO2-associated clonal T cell proliferation in two patients after gene therapy for SCID-X1.* Science, 2003. **302**(5644): p. 415-9.
76. Liu, N., et al., *Stem cell competition orchestrates skin homeostasis and ageing.* Nature, 2019. **568**(7752): p. 344-350.
77. Franzke, C.W., et al., *C-terminal truncation impairs glycosylation of transmembrane collagen XVII and leads to intracellular accumulation.* J Biol Chem, 2006. **281**(40): p. 30260-8.
78. Nanba, D., et al., *EGFR-mediated epidermal stem cell motility drives skin regeneration through COL17A1 proteolysis.* J Cell Biol, 2021. **220**(11).
79. Bonafont, J., et al., *Correction of recessive dystrophic epidermolysis bullosa by homology-directed repair-mediated genome editing.* Mol Ther, 2021. **29**(6): p. 2008-2018.
80. Shy, B.R., et al., *High-yield genome engineering in primary cells using a hybrid ssDNA repair template and small-molecule cocktails.* Nat Biotechnol, 2022.
81. Petković, I., et al., *COL17A1 editing via homology-directed repair in junctional epidermolysis bullosa.* Front Med (Lausanne), 2022. **9**: p. 976604.